miR-542 promotes mitochondrial dysfunction and SMAD activity and is raised in ICU Acquired Weakness

Roser Farre Garros[1], Richard Paul[1,2], Martin Connolly[1], Amy Lewis[1], Benjamin E Garfield[1], S. Amanda Natanek[1], Susannah Bloch[1,2], Vincent Mouly[3] Mark J Griffiths[4], Michael I Polkey[2] and Paul R. Kemp[1]

[1]Molecular Medicine Section, National Heart & Lung Institute, Imperial College, South Kensington Campus, London SW7 2AZ, UK

[2]National Institute for Health Research Respiratory Biomedical Research Unit at Royal Brompton and Harefield NHS Foundation Trust and Imperial College, London, London SW3, 6NP, UK

[3]Sorbonne Universités, UPMC Univ Paris 06, INSERM UMRS974, CNRS FRE3617, Center for Research in Myology, 47 Boulevard de l'hôpital, 75013 Paris, France

[4]Inflammation, Repair and Development, National Heart & Lung Institute, Imperial College, South Kensington Campus, London SW7 2AZ, UK

Running title: Role of miR-542 in ICU acquired weakness

Corresponding author: Dr Paul Kemp,

Molecular Medicine Section, National Heart & Lung Institute, Imperial College, South Kensington Campus, London SW7 2AZ, UK

Email: p.kemp@imperial.ac.uk

Tel : 020 7594 1716

Author Contributions: The overall study was designed by PK with contributions from MG, MIP and AL. Patients were recruited and samples were collected by RP, SAN, and SB. The laboratory studies were performed by RFG, RP, MC, AL, BG, PK and JYL. VM isolated the human muscle cell line. PK wrote the first draft of the paper and all authors provided critical appraisal and input into the manuscript.

At a Glance Commentary

Scientific Knowledge of the Subject

Muscle dysfunction associated with critical illness, Intensive Care Unit Acquired Weakness (ICUAW), is a common complication that has profound prognostic and economic implications. The mechanisms that result in muscle dysfunction are not fully understood but a loss of mitochondrial function and increased atrophic signalling contribute to muscle dysfunction. microRNAs are critical regulators of cell phenotype, so are likely to be important contributors to muscle wasting.

What this study adds to the field

miR-542-3p and -5p were increased in the quadriceps of patients with ICUAW. Increased miR-542-3p targets mitochondrial ribosomal proteins, reducing mitochondrial translation and leading to mitochondrial dysfunction *in vitro* and *in vivo*. Increased miR-542-5p promoted SMAD signalling and reduced the expression of SMAD7, SMURF1 and SMAD phosphatases *in vitro* and in an animal model. This study therefore identifies miR-542-3p and -5p as mediators of mitochondrial and muscle dysfunction in ICUAW.

Abstract

Rationale: Loss of skeletal muscle mass and function is a common consequence of critical illness and a range of chronic diseases but the mechanisms by which this occurs are unclear.

Objectives: We aimed to identify miRNAs that were increased in the quadriceps of patients with muscle wasting and to determine the molecular pathways by which they contributed to muscle dysfunction.

Methods: miR-542-3p/-5p were quantified in the quadriceps of patients with COPD and intensive care unit acquired weakness (ICUAW). The effect of miR-542-3p/5p was determined on mitochondrial function and TGF-β signaling *in vitro* and *in vivo.*

Measurements and main results: miR-542-3p/5p were elevated in patients with COPD but more markedly in patients with ICUAW. *In vitro,* miR-542-3p suppressed the expression of the mitochondrial ribosomal protein MRPS10, and reduced 12S rRNA expression suggesting mitochondrial ribosomal stress. miR-542-5p increased nuclear phospho-SMAD2/3 and suppressed expression of SMAD7, SMURF1 and PPP2CA, proteins that inhibit or reduce SMAD2/3 phosphorylation suggesting that miR-542-5p increased TGF-beta signaling. In mice, miR-542 over-expression caused muscle wasting, reduced mitochondrial function, 12S rRNA expression and SMAD7 expression, consistent with the effects of the miRNAs *in vitro*. Similarly, in patients with ICUAW, the expression of 12S rRNA and of the inhibitors of SMAD2/3 phosphorylation were reduced, indicative of mitochondrial ribosomal stress and increased TGF-β signaling. In patients undergoing aortic surgery, pre-operative levels of miR-542-3p/5p were positively correlated with muscle loss following surgery.

Conclusion; Elevated miR-542-3p/5p may cause muscle atrophy in ICU patients through the promotion of mitochondrial dysfunction and activation of SMAD2/3 phosphorylation.

Introduction

Admission to the intensive care unit is often accompanied by a marked loss of skeletal muscle mass and function (1) that extends weaning time (2) and leads to a reduction in quality of life and an increase in mortality (3, 4). Recovery from muscle wasting can be very slow with many patients still having reduced function 5 years after critical illness (5). Muscle dysfunction also occurs in a number of chronic diseases including COPD contributing to increased morbidity and mortality (6). Skeletal muscle loss occurs as a result of an imbalance between protein synthesis and breakdown, with similar signaling pathways being implicated. For example, increased GDF-15 and reduced IGF-1 have been reported in both critical illness and COPD (7-10). In addition to occurring as a consequence of muscle loss, decreased function also results from a reduction in the muscles' capacity to generate ATP, associated with a reduction in the activity of mitochondrial protein complexes, notably complexes I, III and IV (11-13). These complexes contain proteins encoded by mitochondrial DNA that require translation by mitochondrial ribosomes.

Although muscle mass and oxidative capacity are primarily thought to be controlled by separate processes (protein and mitochondrial turnover), they are to some extent interdependent, since increasing oxidative capacity requires protein synthesis and increasing protein synthesis requires energy. Similarly, reducing oxidative capacity requires protein breakdown and autophagy, processes that operate during muscle breakdown. It is perhaps therefore not surprising that the loss of muscle mass and oxidative capacity often occur together (14) raising the possibility that there are common regulatory mechanisms or factors. Understanding such factors is important in identifying novel therapeutic approaches to treating muscle dysfunction.

MicroRNAs (miRNAs) are small RNAs that control the translation and degradation of sets of mRNAs, modulating biological responses and cell phenotype by regulating the levels of key proteins in multiple biological pathways. For example, miR-1 is elevated during muscle differentiation and regeneration (15), contributing to myogenesis both by suppressing the expression of HDAC4 (an

inhibitor of a number of myogenic transcription factors) and by entering mitochondria and increasing mitochondrial translation (16). Consistent with this, we and others have previously reported reduced expression of miR-1 is associated with muscle wasting in COPD (17), renal failure (18) and intensive care unit acquired weakness (ICUAW) (7) , although there is some discrepancy in the COPD literature (10). We have also identified a miRNA pattern associated with muscle mass in COPD patients that is distinct from that in healthy individuals (19). The miRNAs identified were associated with pluripotency and regeneration, indicating that patients who lost the most muscle were unable to respond sufficiently to the physiological stress imposed by disease. This observation suggests that some patients are more susceptible to muscle atrophy in the presence of disease but does not identify factors associated with disease that drive the loss of muscle, nor did the miRNA pattern identified associate with the loss of oxidative capacity. Consequently, we hypothesised that there would be changes in miRNA expression in the quadriceps of COPD patients that promoted atrophy and a loss of oxidative capacity. In this study, we therefore reanalysed our screen to identify miRNAs associated with COPD that were predicted to target pathways controlling protein turnover and energy balance; miR-542-3p and -5p fulfilled these criteria (mitochondrial translation and TGF-β signaling respectively). However analysis of the expression of these miRNAs in patients with established ICUAW showed that they were more markedly increased in those patients than in COPD patients, consistent with the more rapid muscle atrophy that these patients undergo. We confirmed the ability of these miRNAs to target the appropriate biochemical pathways both *in vitro* and *in vivo* and showed that expression of the miRNA could cause muscle wasting *in vivo*. Finally, we analysed the expression of these miRNAs in the response of patients to the insult of aortic surgery, which we have characterised as a human model of ICUAW (8). Some of the results of these studies have been previously reported in the form of an abstracts (20-22)

Methods

Subjects

COPD cohort: Stable patients with COPD according to the Global Initiative in Obstructive Lung Disease (GOLD) guidelines 2004 (23) were enrolled from clinics at the Royal Brompton Hospital. Exclusion criteria are described in the supplement. Healthy age-matched controls were recruited by advertisement. COPD subjects in this study form part of a larger well-phenotyped cohort described by Natanek *et al* (14). Samples from 14 patients and 7 controls were used in the initial miRNA screen. The validation cohort included samples from 24 patient and 12 controls none of which formed part of the screen. Demographic data for these patients are shown in Supplemental Tables 1 and 2.

Physiological measurements: Details of the methods used to assess physiological parameters (body composition, lung function, physical performance and strength) are given in the supplement. Muscle biopsy was performed by percutaneous needle biopsy in the mid-thigh of the *vastus lateralis,* of the same leg in which strength had been tested, under local anaesthesia using the Bergstrom technique (24).

Intensive Care unit acquired weakness (ICUAW) cohort: This cohort (17 patients with ICUAW and 7 controls) has been described previously (7) and recruitment details are given in the supplement. The muscle biopsies were taken from the *rectus femoris* by the Bergstrom technique (24) or as open biopsies. There was no difference between patients and controls in age (62 ± 18 and 68± 11 yrs) nor in BMI (27.8 ± 3.9 and 25.2± 3.8 kg/m^2).

Aortic surgery cohort: Patients provided written informed consent and the study was approved by the National Research Ethics Committee (study 13/LO/0479). Patients undergoing elective cardiothoracic surgery at Royal Brompton Hospital were recruited. The principal inclusion criterion was a high-risk elective aortic surgical procedure requiring admission to the ICU. Pre-surgical exclusion criteria included pre-existing muscular or neuromuscular disease, malignancy,

contraindication to muscle biopsy. Patients were also excluded if clinical instability precluded a biopsy after surgery. *Rectus femoris* cross sectional area (RF_{CSA}) was determined by ultra-sound prior to surgery and 7 days after surgery, as previously described (25). An open biopsy was taken after the induction of anaesthesia but before the start of surgery from the *rectus femoris* and a second biopsy was taken using the Bergstrom technique 24h after surgery. Blood samples were collected prior to surgery and regularly during the first 7 days after surgery. Demographic data for these patients are shown in Supplemental Table 3.

Quantification of RNA and protein in biological samples*:* Details of the analysis methods for RNA and protein have been described before and are detailed in the supplement.

In vitro and animal experiments: Targets of miR-542-3p/5p were identified by Ago-2 pull down. The effects of the miRNAs on gene and protein expression, as well as on mitochondrial function and TGF-β signaling were determined in LHCN-M2 cells, a human skeletal muscle cell line. Over-expression of the miRNA in mouse muscle was achieved by electroporation of an EGFP-miRNA construct (pCAGGS-miR-542). Experimental procedures for the *in vitro* and animal experiments are detailed in the supplement.

Statistical analysis: Gene expression data were log transformed to produce normal distribution and stabilise variance. Person correlations were performed for correlation analysis assuming linearity *(Aabel).* Differences between groups were calculated using Student's t-test for normally distributed data or by Mann-Whitney U test for non-parametric data *(Aabel)*. *In vitro* data shown were produced in three independent experiments, for gene expression data and luciferase assays treatments were performed in sextuplet within each experiment.

Results

Analysing our original screen (19) of 14 male patients with GOLD 3-4 COPD and 7 age matched healthy male controls to identify miRNAs associated with disease showed that 26 miRNAs were suppressed at $p<0.01$ (Table 1). The most statistically significantly down-regulated miRNAs were miR-144 and miR-499. Only 6 miRNAs were increased in the muscle of COPD patients, 5 of which (miR-542-5p, miR-542-3p, miR-424, miR-424* and mir-450a) came from a single locus on the X-chromosome. The most upregulated miRNA from this cluster was miR-542-5p and the miRNA showing the most significant increase was miR-542-3p. Analysing the expression of miR-542-3p in a larger cohort of male controls and patients with the same inclusion criteria (n=12 controls and n=24 COPD patients) confirmed the elevation of miR-542-3p 2 fold ($p=0.012$, Fig. S1) indicating that the finding was robust.

We had previously shown similar changes in miR-499 in patients with ICUAW (7), so we determined whether miR-542-3p and -5p were increased in samples from the same patients and found that they were markedly more elevated than in the COPD patients (15 fold and 50 fold, respectively) (Fig. 1 A, B) and correlated with length of hospital stay (Fig. 1 C, D). Moreover miR-542-5p was higher in those with a sequential organ failure assessment (SOFA) score at the time of biopsy > 10 than in patients with a SOFA score < 10 (Fig. 1E, F).

miR-542-3p promotes mitochondrial ribosomal stress

For these miRNAs to be important regulators of muscle phenotype in disease they must target appropriate biochemical pathways. Bioinformatic analysis using miRwalk (26) showed that miR-542-3p may target components of the mitochondrial ribosome including mitochondrial ribosomal protein (MRP)S2, S10, S18C, S25, S26 and S27 so may induce mitochondrial ribosomal stress, thereby reducing the expression of mitochondrially encoded proteins, which would be expected to reduce mitochondrial function including energy production. Similar analysis showed that miR-542-5p would target inhibitors of the TGF-β signaling pathway, which is known to mediate muscle atrophy,

suggesting that it may increase TGF-β signaling. Hence miR-542-3p/5p are predicted to target pathways that affect both muscle mass and function.

Ago-2 pull-down followed by qPCR showed enrichment of all the MRPs tested (MRP S2, S27, S18C and S10) in RNA isolated from miR-542-3p transfected cells compared to cells transfected with control miRNA (Fig. S2A). To determine whether these interactions resulted in reduced mitochondrial ribosomal protein and thereby suppressed mitochondrial translation, we quantified the expression of one target (MRPS10) and one product of mitochondrial protein synthesis (Cytb5). Protein levels of MRPS10 were reduced in response to transfection with miR-542-3p by 50%. Cytb5 protein levels were also reduced but to a much smaller extent (Fig. 2 A-C). Transfection with miR-542-3p also reduced the mitochondrial membrane potential measured using Mitotracker® Red and JC1 (Figs 2D and S2B). Both effects were reversible by cotransfection with the antagomiR (Figs 2D and S2C). There was no effect of the miRNA on the amount of mitochondrial DNA relative to nuclear DNA, indicating that the results were not due to a reduction in mitochondrial content.

Ribosome stress induced by reduced small subunit proteins is accompanied by a decrease in ribosomal RNA especially the small subunit RNA (27). Consistent with the induction of ribosome stress, miR-542-3p suppressed the expression of the 12S rRNA to a greater extent than the 16S rRNA (mitochondrial rRNAs from the small and large subunits respectively) and these changes were reversible with an antagomiR (Fig 2E).

miR-542-5p causes ligand independent SMAD2/3 phosphorylation and suppresses SMAD7 *in vitro*

Bioinformatic analysis predicted that miR-542-5p targets a number of components of the TGF-β family signaling pathway, including SMAD7 and SMURF1 (which inhibit the TGF-β type I receptor (28)), and the proteins that dephosphorylate and inactivate the SMAD2/3 complex (PPP2CA supplementary results and Fig. S3). Ago2 pull-down and qPCR confirmed enrichment for SMURF1 and PPP2CA (Fig. S3A) but SMAD7 mRNA expression was too low to prove targeting.

The effect of miR-542-5p on TGF-β signalling was determined using a SMAD dependent luciferase reporter (29). In the absence of exogenous ligand, miR-542-5p increased luciferase activity 2 fold (ANOVA $p<0.001$, Fig.3B). Furthermore, transfection of cells with a dominant inhibitory form of the TGFβ type II receptor inhibited the effects of the miRNA suggesting that a functional receptor complex was required for the response (Fig. 3C). After phosphorylation, SMAD2/3 translocates to the nucleus and, consistent with the increase in basal SMAD dependent luciferase activity, immunofluorescence assay showed increased nuclear pSMAD2/3 in cells transfected with miR-542-5p compared to scrambled miRNA (ANOVA $p<0.001$, Fig. 3D, E and S4). Western blotting confirmed increased pSMAD2/3 in the presence of miR-542-5p (Fig. S4).

To determine which predicted targets of miR-542-5p were suppressed, the mRNAs for SMAD7, SMURF1 and PPP2CA were quantified by PCR. miR-542-5p suppressed the expression of all components (Fig 4A). SMAD7 expression was not readily detectable by western blotting in LHCN-M2 cells, but was detectable by immunoprecipitation, which demonstrated that miR-542-5p suppressed the expression of SMAD7 (Fig. 4B and C) suggesting that SMAD7 is targeted by the miRNA. However, as we could not confirm an interaction between the miRNA and SMAD7 mRNA this reduction in may be indirect.

Over-expression of miR-542 promotes mitochondrial dysfunction, suppresses SMAD7 and causes atrophy *in vivo*

To determine whether the effects of miR-542-3p and -5p observed *in vitro* could also occur *in vivo* and to determine whether it could cause atrophy, miR-542 was overexpressed in the *tibialis anterior* of mice by electroporation with positively transfected fibres identified by co-expression of EGFP and compared to expression of EGFP alone. Three days after electroporation, 37% of the fibres expressed detectable EGFP (38% EGFP only leg and 36% miR-542 leg, Fig S5). miR-542-3p levels were 10 fold higher than in the control leg ($p=0.04$ paired t-test). The miR-542 expressing muscle was smaller than the contralateral muscle expressing EGFP alone (Fig. 5A). The average diameter of

transfected, EGFP expressing, fibres in the miR-542 transfected leg were smaller than the untransfected fibres in the same leg (Fig. 5B and Fig. S5A). There was no difference in size between the transfected and untransfected fibres in the muscle of the control transfected leg, nor between the untransfected fibres in the two muscles. Quantification of mitochondrial complex I activity (the first component of the electron transport chain) showed a marked reduction in the muscles expressing the miRNA compared to those expressing the EGFP alone (Fig 5C). Similarly, JC-1 staining of the mitochondria showed a reduction in mitochondrial membrane potential (Fig 5D). As the electroporation does not transfect all of the tissue, we enriched the samples by laser capture microdissection to quantify the expression of rRNAs in transfected fibres. This analysis showed a significant reduction in 12S rRNA in fibres expressing EGFP and miR-542 compared to those expressing EGFP alone that was greater than any reduction in 16S rRNA consistent with mitochondrial ribosomal stress (Fig. 5E). Quantification of SMAD7 protein also showed a marked downregulation of the protein in the miR-542 expressing leg (5F and S5).

Patients with ICUAW show reduced expression of 12S rRNA and inhibitors of TGF-β signaling

Mitochondrial rRNAs and SMAD7, SMURF1, and PPP2CA were analysed in patients with ICUAW to determine whether a similar pattern of changes occurred. Both the 12S and 16S rRNAs were reduced but the reduction in 12S rRNA was larger resulting in a significant reduction in the 12S:16S ratio (Fig. 6 A-C) consistent with the *in vitro* and *in vivo* findings. Furthermore the expression of SMURF1, and PPP2CA were reduced at the mRNA level (Fig 7A), and both mRNA and protein levels of SMAD7 were reduced (Fig 7B, C). Our previous analysis of the ICUAW cohort samples analysed here, showed that patients with established ICUAW have higher nuclear pSMAD2/3 and increased expression of Cyr-61, a TGF-β responsive gene (7). These data are consistent with mitochondrial ribosome stress and increased TGF-β signaling in the patients.

miR-542-3p/5p is associated with muscle loss following cardio-pulmonary bypass surgery

Half of patients admitted to the ICU following aortic surgery lose more than 10% of their RF_{CSA} over the subsequent 7 days (8). We therefore quantified change in muscle size over 7 days in a separate cohort of 40 patients in whom we also took muscle biopsies immediately prior to surgery (Table S3). Nineteen of these patients lost more than 10% RF_{CSA} following surgery. Pre-surgery expression of miR-542-3p and -5p were weakly associated with pre-surgery left ventricular ejection fraction (LVEF%, Fig. 8 A, B).

The preoperative expression of miR-542-3p and -5p was higher in patients who lost more than 10% RF_{CSA} in the 7 days following surgery than in those who lost less than 10% RF_{CSA} (Fig. 8 C, D). Furthermore, preoperative expression of these miRNAs correlated with the amount of muscle lost (Fig. 8 E, F) and length of hospital stay (Fig S6 A, B). Age and preoperative LVEF% were also associated with muscle loss after surgery (Fig. S7). However, in multiple regression analysis using LVEF%, age and either miR-542-3p or miR-542-5p expression prior to surgery, only the miRNAs were retained as having a significant association.

Discussion

ICUAW has a significant impact on patient mortality and morbidity, as well as on the economics of critical illness. A range of different factors (including oxidative stress, sepsis, and growth factor dysregulation (30)) mediate ICUAW by interfering with intracellular processes. Our data show that quadriceps expression of two microRNAs, miR-542-3p/5p, which are predicted to target processes essential for muscle maintenance, is markedly elevated in patients with established ICUAW suggesting that these miRNAs contribute to the wasting process. The *in vitro* studies confirm that miR-542-3p/5p regulate appropriate pathways (mitochondrial function and SMAD2/3 signaling) in a manner that would contribute to wasting. Furthermore, over-expression of miR-542, to a similar

fold change as that seen in patients with ICUAW, caused muscle wasting and mitochondrial dysfunction in mice. Finally we show that in patients admitted to the ICU following aortic surgery, the level of expression of miR-542-3p/5p at the time of surgery is associated with muscle wasting in the 7 days following surgery. Consequently, we have demonstrated that the expression of specific miRNAs is associated with wasting in humans, identified mechanisms by which they may promote wasting and demonstrated that they can cause wasting in mice.

miR-542-3p and mitochondrial dysfunction

Reduced mitochondrial number and mitochondrial dysfunction have been previously demonstrated in the quadriceps of patients on the ICU (31). Indeed mitochondrial dysfunction has been suggested as a mechanism leading to the metabolic failure associated with ICUAW (32). One feature of the reported mitochondrial dysfunction in ICUAW is a reduction in the activity of electron transfer complexes that require mitochondrially translated proteins (notably complex I, III and IV (11, 12)). Reduced activity of these complexes as a consequence of mitochondrial ribosomal stress is also found in individuals born with mutations in MRPS16 and MRPS22 (33, 34). The identification here of a miRNA that promotes mitochondrial ribosomal stress (as identified by the reduction in MRPS10, 12S rRNA and mitochondrial membrane potential), together with the demonstration of a reduction in the 12S to 16S rRNA ratio in patients with established ICUAW suggest two novel findings; firstly that mitochondrial ribosomal stress contributes to metabolic failure and wasting in ICUAW, and secondly that elevated miR-542-3p is a contributor to this process. At first glance, there is a discrepancy between our data and that of Fredriksson *et al* who showed no decrease in mitochondrial protein synthesis in patients with ICUAW (35). However, in that study they measured protein synthesis from whole mitochondria. The majority of proteins in mitochondria are encoded by nuclear genes, translated in the cytoplasm and imported into mitochondria with only 13 proteins translated by mitochondrial ribosomes. Consequently, whilst their experiment demonstrates no change in the synthesis of mitochondrial proteins it does not measure the rate of translation within

mitochondria of key components of the complexes involved in oxidative phosphorylation as the bulk of the proteins assayed will have been synthesised in the cytoplasm.

miR-542-5p and TGF-β signaling

Myostatin is an important regulator of muscle mass that promotes phosphorylation of SMAD2/3. Inhibiting the myostatin pathway and thereby suppressing SMAD2/3 phosphorylation has been suggested as a means of treating ICUAW (www.clinicaltrials.gov reference NCT01321320). However, circulating levels of myostatin did not increase in patients admitted to the ICU following aortic surgery (8). Our studies suggest that increased expression of miR-542-5p contributes to muscle wasting by promoting SMAD2/3 phosphorylation, a down-stream effect of myostatin binding to TGF-β receptors, thereby potentially bypassing the need for significantly elevated myostatin. The effect of the dominant inhibitory receptor, together with inability of miR-542-5p to increase luciferase activity in the presence of 5ng/mL TGF-β indicate that miR-542-5p is not acting via a separate pathway as the effects are not additive. Our data indicate that miR-542-5p increases pSMAD2/3 by suppressing the inhibitory components of the TGF-β signaling pathway with a reduction in the expression of the SMAD7 and SMURF1, inhibitors of TGF-β type I receptors, as well as of the phosphatases that limit TGF-β signaling by dephosphorylating and inactivating SMADs. Our observation that the increase in luciferase activity in the absence of exogenous ligand was inhibited by the dominant inhibitory receptor suggests that it occurs as a result of either low level receptor kinase activity in the absence of ligand or a sensitisation of the signal to the low levels of TGF-β receptor ligands present in the serum used to culture the cells or produced by the cells themselves.

Our previous analysis of the samples from the ICUAW cohort analysed here showed that patients with established ICUAW have higher nuclear pSMAD2/3 and increased expression of Cyr-61, a TGF-β responsive gene (7). Here we show that these patients also have increased miR-542-5p, alongside reduced expression of SMAD7, SMURF1 and PPP2CA suggesting that these factors contribute to the observed increases in TGF-β signaling.

miR-542-5p is not the only miRNA from this locus to target components of the TGF-β signaling pathway. For example, miRNAs from the miR-424-503 polycistron reduce SMAD7 and promote TGF-β signaling (36). Furthermore, as these miRNAs are also regulated by TGF-β signaling it is possible that they form part of a positive feedback loop (37). It seems likely therefore that increased expression of these miRNAs also contributes to elevated TGF-β signaling and atrophy in ICUAW.

miR-542 and muscle atrophy

The combined effects of miR-542 on mitochondrial function and TGF-β signaling suggest that it contributes to muscle wasting and dysfunction. We confirmed the potential of these miRNAs to promote wasting by over-expression in the muscle of mice. This over-expression caused marked muscle loss within 3 days that was accompanied by mitochondrial dysfunction and reduced SMAD7 expression, demonstrating the potential of miR-542 to drive atrophy. This loss of muscle is larger and more rapid than that achieved by over-expression of myostatin or GDF-15 using the same promoter as used here (9, 38).

Clinical Implications

The data presented here identify miR-542-3p/5p as potential therapeutic targets in patients with ICUAW. Therapy could take the form of antagomiRs for miR-542-3p/5p or the suppression of the mechanisms that drive the expression of the miRNAs. The data also show that some aspects of the propensity to waste are established in patients before they become critically ill because patients with the highest pre- aortic surgery miR-542 levels wasted more than those with the lowest, raising the possibility that a therapy could be given to vulnerable patients prior to major surgery. In addition, pre-operative miR-542 levels could be used to stratify patients in high or lower risk of peri- and post-operative muscle atrophy so that high-risk patients could have intensive nutritional and rehabilitation input. Since we identified miR-542 as being elevated in COPD and as the expression of this miRNA was associated with LVEF in our aortic surgery patients, it is possible that this miRNA locus contributes to muscle wasting in a wider range of conditions but that its effects are greatest

with the insults imposed as a result of critical illness. Contributing to both chronic and acute wasting is not without precedent since many pathways including GDF-15 and IGF-1 have been associated with both chronic and acute wasting (8-10). Furthermore, the pathways leading to muscle loss are common with a suppression of protein synthesis relative to degradation and mitochondrial dysfunction being end components.

Critique of the study

The study presents a cross sectional analysis demonstrating elevation of miR-542-3p/5p in ICUAW and a longitudinal study showing an association of these miRNAs with muscle loss after surgery. We cannot therefore directly demonstrate that elevation of the miRNA causes either the reduction in oxidative capacity or promotes the loss of muscle mass in humans. However, the demonstration that the miRNAs cause appropriate biochemical changes *in vitro*, muscle wasting in mice, and the demonstration of appropriate phenotypic manifestations in humans strengthens our conclusions.

Conclusion

Our data indicate that expression of miR-542-3p/5p is elevated in patients with ICUAW. These miRNAs target the synthesis of mitochondrial ribosomal proteins and of inhibitors of TGF-β signaling. In mice their over-expression promotes mitochondrial dysfunction and muscle wasting. Elevation of these miRNAs in the muscle of ICUAW patients is a very plausible mechanism contributing to the loss of oxidative capacity and muscle wasting observed in this condition.

Acknowledgements

This work was supported by the MRC COPDMAP, the British Heart Foundation and the NIHR Respiratory Disease Biomedical Research Unit at the Royal Brompton and Harefield NHS Foundation Trust and Imperial College London who part funded MIP's salary and wholly funded RFG and AVD.

The views expressed in this publication are those of the authors and not necessarily those of the NHS, The National Institute for Health Research or the Department of Health. AL received a BBSRC funded studentship and was later funded by COPDMAP. JL was wholly supported by COPDMAP. SB was supported by an MRC clinical Research Fellowship. MC is supported by a BHF studentship. The LHNC-M2 cells were derived using the platform for immortalization of human cells from the Myology Institute in Paris.

Figure Legends

Figure 1. miR-542-3p/5p are increased in patients with ICUAW and are associated with length of ICU stay

miR-542-3p/5p were quantified in quadriceps biopsies from patients (n=17) with established ICUAW and pre-operative controls (n=7). Box and whiskers plots showing that the expression of miR-542-3p (A) and miR-542-5p (B) are increased in patients compared to controls ($p<0.001$ and $p<0.001$ respectively, whiskers to 90% with outliers shown). In patients with ICUAW, miR-542-3p (C) and miR-542-5p (D) expression were positively correlated with length of ICU stay ($r=0.58$, $p=0.014$ and $r=0.57$, $p=0.016$ respectively). miR-542-5p (F) but not miR-542-5p (E) was increased in patients with a SOFA score > 10 on the day of biopsy compared to those with a SOFA score <10.

Figure 2. miR-542-3p promotes mitochondrial ribosomal stress and inhibits mitochondrial function *in vitro*

LHCN-M2 cells were transfected with scrambled mimic (scr), miR-542-3p (542-3p), or miR-542-3p in the presence of its antagomiR (542-3p + ant). Transfected miR-mimic levels were kept constant in all experiments by co-transfection with scr. 48h later protein or RNA were extracted or the mitochondrial membrane potential was measured as described in Methods. Levels of the miR-542-3p target, MRSP10, and the mitochondrially encoded CytB were lower in miR-542-3p transfected cells (A-C). miR-542-3p suppressed 12S and 16S (D) rRNA compared to scrambled miRNA and this effect was reversed by the antagomiR. miR-542-3p suppressed mitochondrial membrane potential measured by JC-1 fluorescence ration and this effect was reversed by the antagomiR (E).

Figure 3. miR-542-5p increases basal SMAD2/3 activity

(A) LHCN-M2 myoblasts were transfected with miR-542-5p mimic or scrambled control then with $CAGA_{12}$ luciferase reporter and pRLTK 24h later as described in Methods. After 24h the cells were treated with vehicle or 5ng/mL TGF-β for 2h. miR-542-5p increased $CAGA_{12}$ promoter activity (p=0.002, t-Test) in the absence of TGF-β but did not further increase TGF-β stimulated $CAGA_{12}$ promoter activity in the presence of 5ng/mL TGF-β (n=6 samples repeated in 2 independent experiments). (B) LHCN-M2 myoblasts were transfected with miR-542-5p mimic or scrambled control then with $CAGA_{12}$ luciferase reporter, pRLTK and either pcDNA3 or a dominant inhibitory form of the TGF-β type II receptor (DNR) in pcDNA3. 24h later the cells were stimulated with 5ng/mL TGF-β for 6h. Expression of the DNR inhibited both TGF-β and miR-542-5p induced increases in luciferase activity (n=6 samples repeated in 3 independent experiments). (C/D) LHCN-M2 myoblasts were transfected with miR-542-5p mimic or scrambled control, cultured for 48h and stained for pSMAD2/3 then treated with TGF-β for 2h. Box and whiskers plot of mean fluorescence in the nuclei from cells transfected with miR-mimic or scrambled control (3 independent experiments). Left-hand images show DAPI staining for nuclei, the right-hand images show pSMAD2/3 staining only. Colour images and a merged view are shown in Fig. S4. p values given for individual t-tests between data sets with a Bonferonni corrected p value for significance =0.0083. Abbreviations: DAPI (4',6-diamidino-2-phenylindole).

Figure 4. **miR-542-5p suppresses the expression of inhibitors of the TGF-β signaling pathway**

(A) LHCN-M2 myoblasts were transfected with miR-542-5p mimic or scrambled control and 48h later RNA was isolated. Messenger RNA for SMURF1, PPP2CA (a catalytic component of PP2A) and SMAD7 were determined. All mRNAs were reduced in miR-542-5p transfected cells compared to those transfected with scrambled controls. Data are from 3 experiments of n=6 per experiment. SMAD7 was immunoprecipitated from LHCN-M2 myoblasts that were left untransfected or were

transfected with miR-mimic or scrambled control and analysed by western blotting. Box and whiskers plot shows mean signal from n=4 independent transfections.

Figure 5. Expression of miR-542 causes muscle wasting, mitochondrial dysfunction and suppression of SMAD7 in mice

The *tibialis anteriors* (TAs) of mice (n=15) were electroporated with an expression vector for EGFP alone (pCAGGS) or with an expression vector for EGFP and miR-542 (pCAGGS-542) as described in Methods in 3 batches of 5 mice. Three days later the mice were sacrificed and the muscle dissected out and weighed. (A) The weight of the TA normalised to bodyweight of the muscle expressing miR-542 was reduced compared to that expressing the EGFP alone ($p=0.016$, n=15 mice, paired t-Test). (B) Fibre diameter was determined for transfected fibres and non-transfected fibres in each leg from the two sets of mice in which the muscles were embedded for sectioning of mice (n=10). Fibres expressing EGFP- and miR-542 were smaller than all other fibres ($p<0.001$ ANOVA) and were smaller than those expressing EGFP alone ($p<0.001$, t-Test). There was no difference in size of the transfected fibres and the untransfected fibres in the pCAGGS electroporated muscles. Cytoplasmic and mitochondrial extracts were made from the second batch of animals and laser capture micro-dissection was performed on the third batch of muscle samples. (C) Expression of miR-542 caused a reduction in both complex I activity (n=4 per group) and (D) mitochondrial membrane potential (assayed by JC-1 fluorescence, n=5 per group) determined in mitochondria isolated from the TA. (E) The expression of the 12S rRNA, measured in RNA isolated from laser capture microdissected tissue, was markedly reduced in muscle fibres expressing miR-542. (F) Immunoprecipitation of SMAD7 from cytoplasmic extracts showed a reduction in SMAD7 expression in muscles expressing miR-542 compared to those expressing EGFP alone ($p=0.004$).

Figure 6. Expression of mitochondrial rRNAs is suppressed in patients with ICUAW.

12S, 16S rRNAs were quantified in RNA samples from the quadriceps of patients with ICUAW. Both 12S and 16S rRNAs were lower in patients with ICUAW compared to controls (A-B). The reduction in 12S rRNA was larger than in 16S rRNA. Consequently the 12S:16S ratio was suppressed in ICUAW patients compared to controls indicative of mitochondrial ribosome stress (C).

Figure 7. Expression of inhibitors of the TGF-β signaling pathway are suppressed in ICUAW

Expression of PPP2CA, SMURF1 and SMAD7 mRNAs was quantified in quadriceps biopsies from patients with ICUAW and controls. All of these inhibitors of the TGF-β signaling pathway were suppressed in patients compared to controls (A). SMAD7 was immunoprecipitated from quadriceps biopsies from patients with established ICUAW or from controls (B) and the intensity of the signals was quantified (C). There was a significant reduction in SMAD7 in the quadriceps of the ICUAW patients.

Figure 8. Levels of miR-542-3p and -5p in the muscle of patients before aortic surgery are associated with post-surgical muscle loss.

miR-542-3p and -5p expression was determined in *rectus femoris* biopsies taken from patients at the time of surgery. Both miRNAs were associated with pre-surgery cardiac function, LVEF% (A and B) [miR-542-3p vs LVEF%; r=-0.43, p=0.005, miR-542-5p vs LVEF%; r=-0.34, p=0.031]. miR-542-3p and miR-542-5p were higher in patients who lost more than 10% of the size of the *rectus femoris* as determined by ultrasound (C, D p=0.018, p=0.023 respectively) and correlated with the amount of muscle lost over the 7 days (r=0.43, 0.006 and r=0.52, p<0.001 respectively). Open circles show patients who lost more than 10%RF_{CSA}, closed circles show patients who lost less than 10%RF_{CSA}.

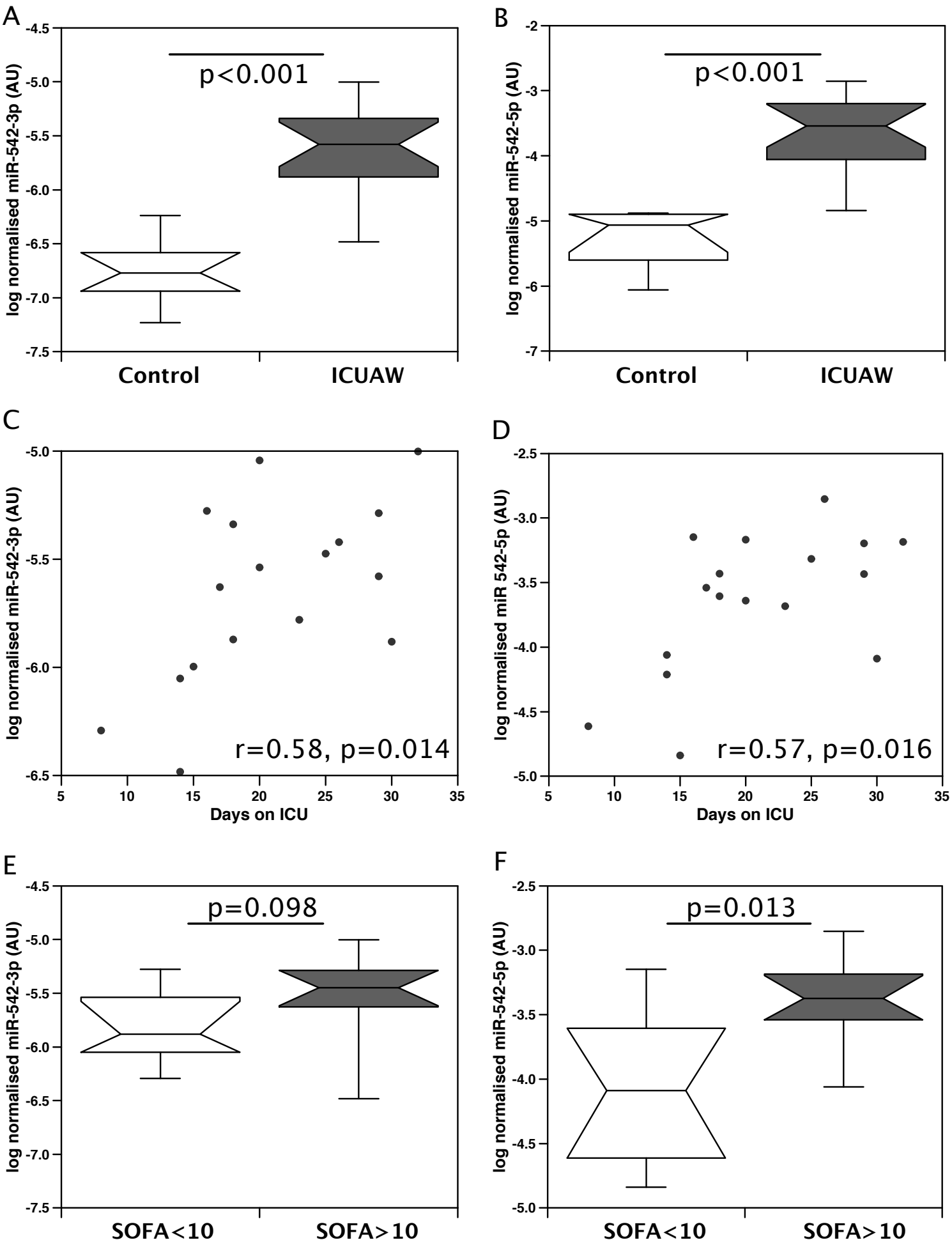
A
log normalised miR-542-3p (AU)
-4.5
-5.0
-5.5
-6.0
-6.5
-7.0
-7.5
p<0.001
Control
ICUAW
B
log normalised miR-542-5p (AU)
-2
-3
-4
-5
-6
-7
p<0.001
Control
ICUAW
C
log normalised miR-542-3p (AU)
-5.0
-5.5
-6.0
-6.5
r=0.58, p=0.014
5
10
15
20
25
30
35
Days on ICU
D
log normalised miR 542-5p (AU)
-2.5
-3.0
-3.5
-4.0
-4.5
-5.0
r=0.57, p=0.016
5
10
15
20
25
30
35
Days on ICU
E
log normalised miR-542-3p (AU)
-4.5
-5.0
-5.5
-6.0
-6.5
-7.0
-7.5
p=0.098
SOFA<10
SOFA>10
F
log normalised miR-542-5p (AU)
-2.5
-3.0
-3.5
-4.0
-4.5
-5.0
p=0.013
SOFA<10
SOFA>10

Figure 1

A

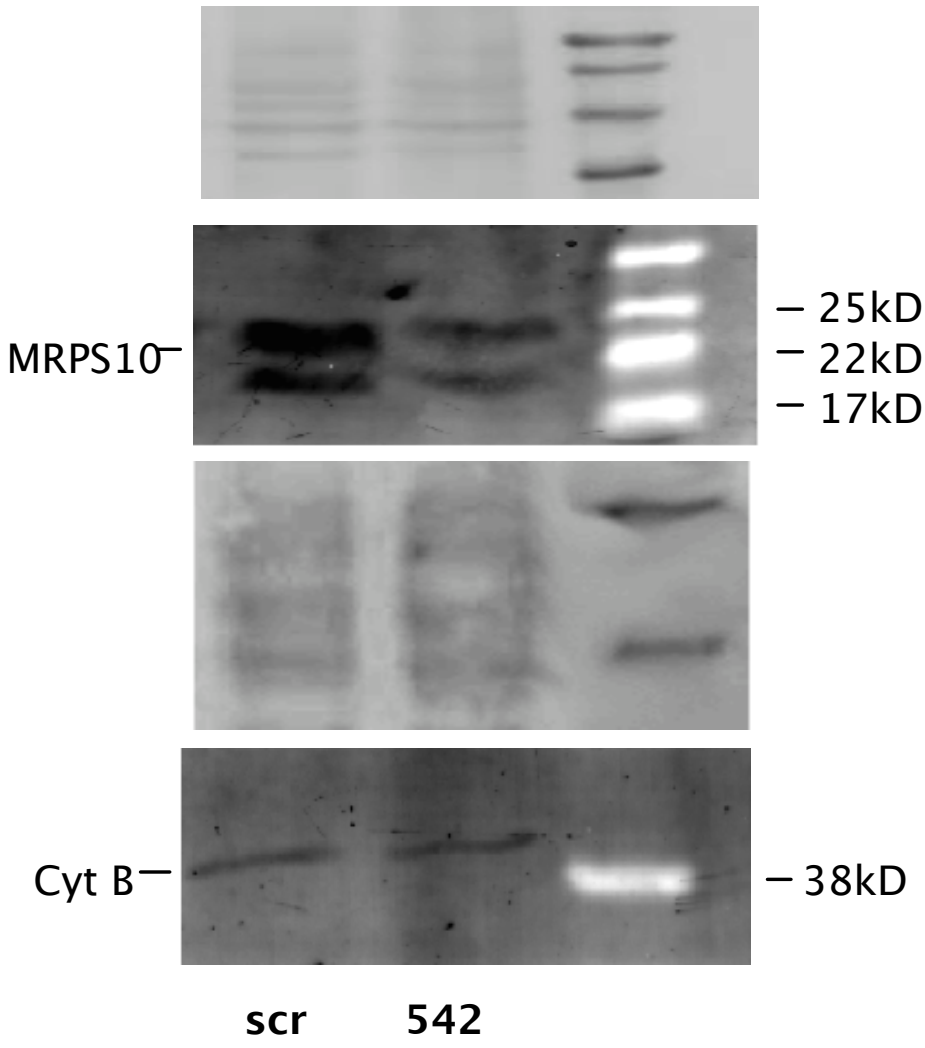

B

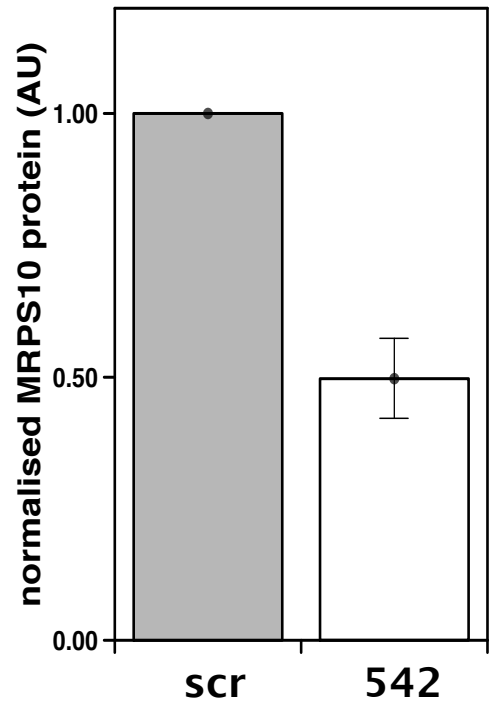

C

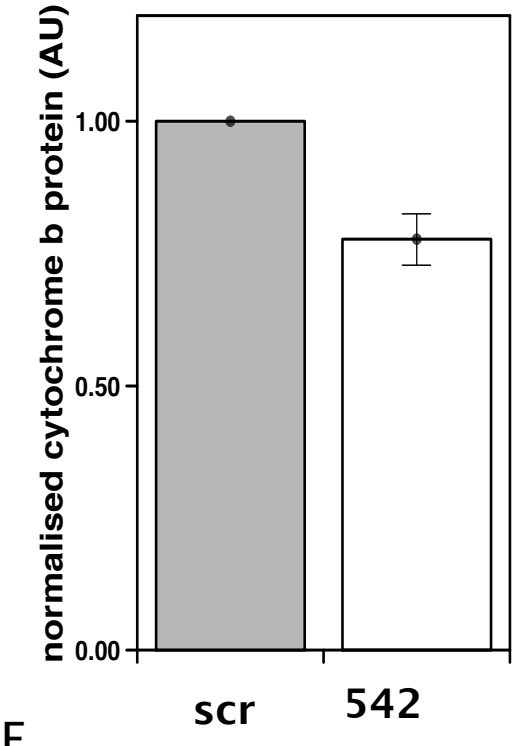

D

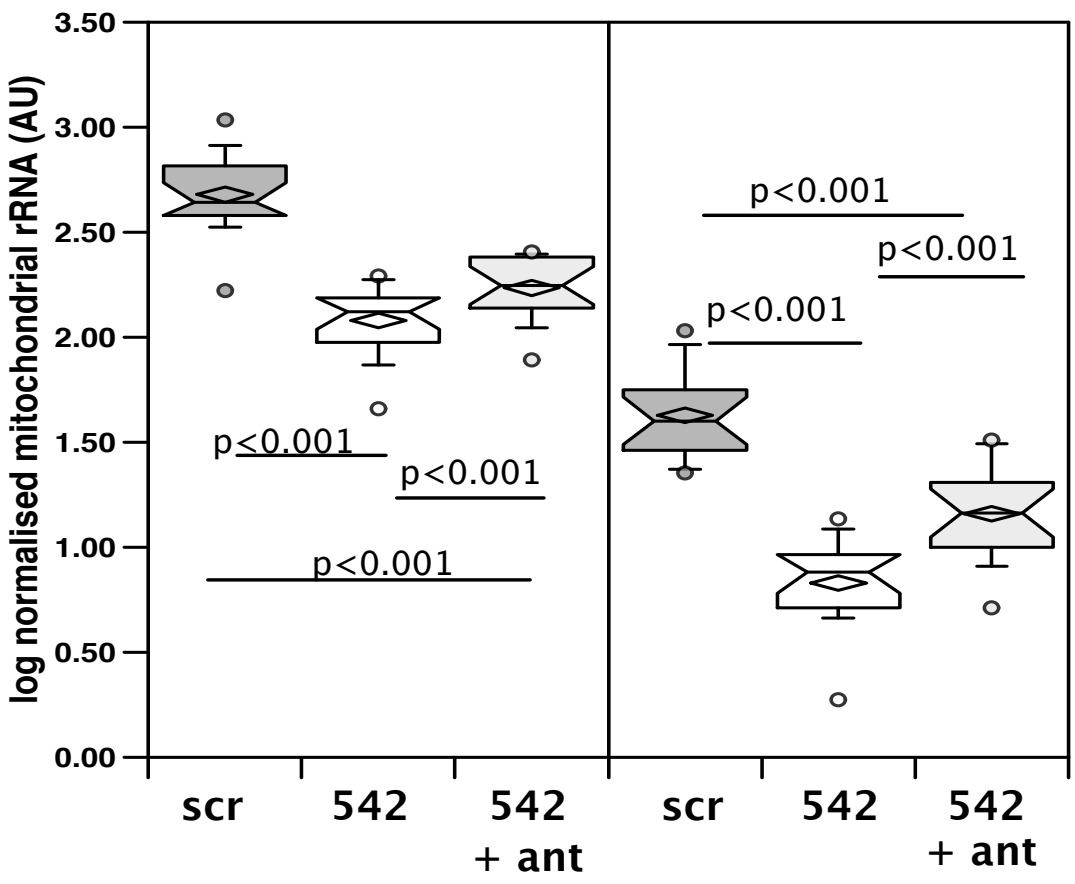

E

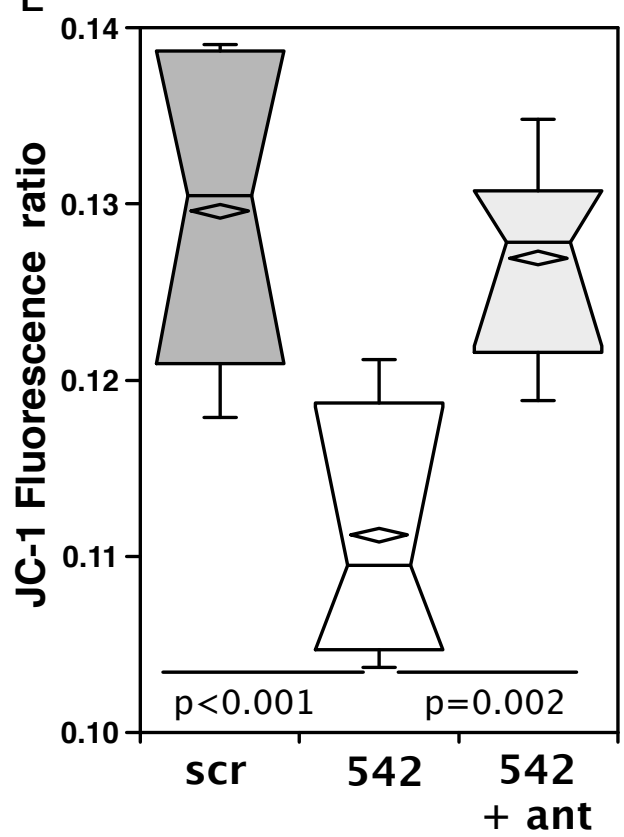

Figure 2

A

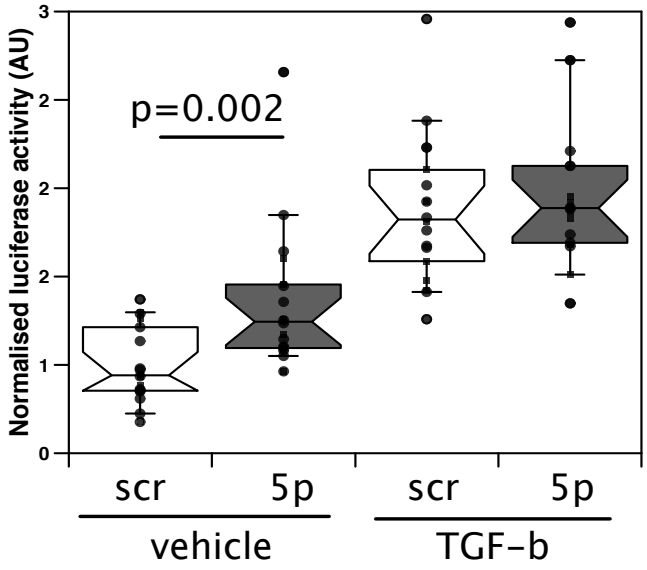

B

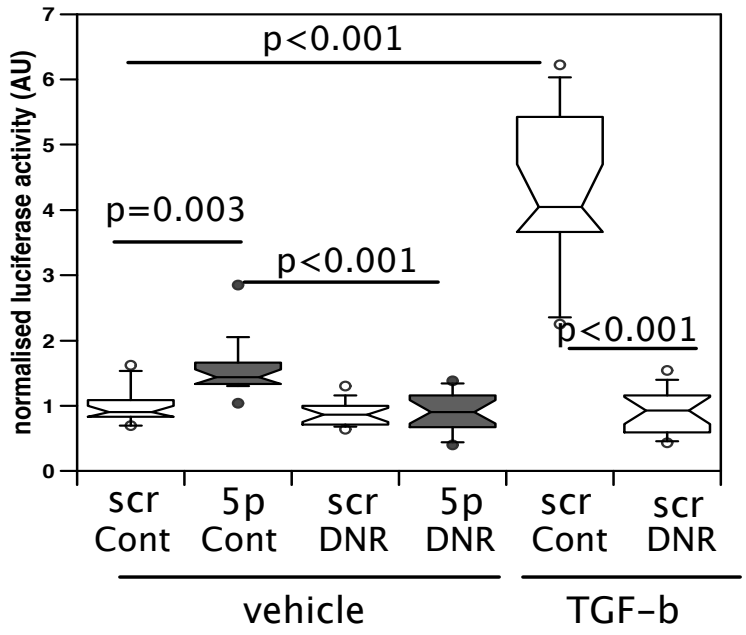

C

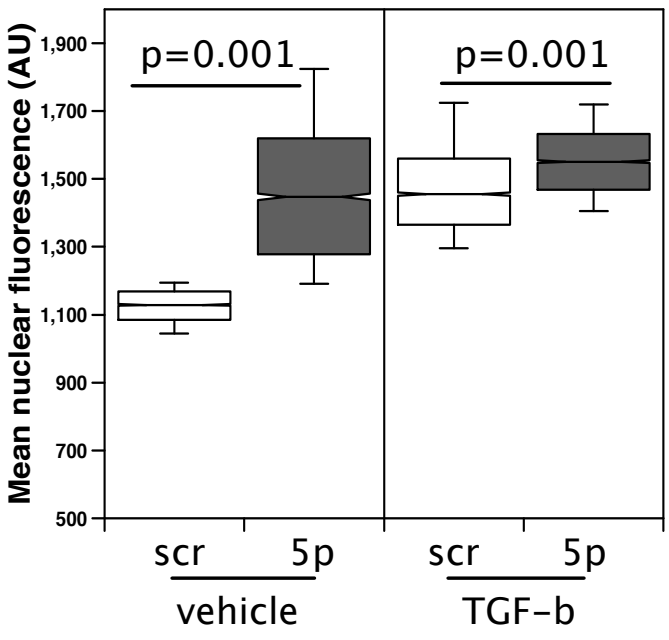

D

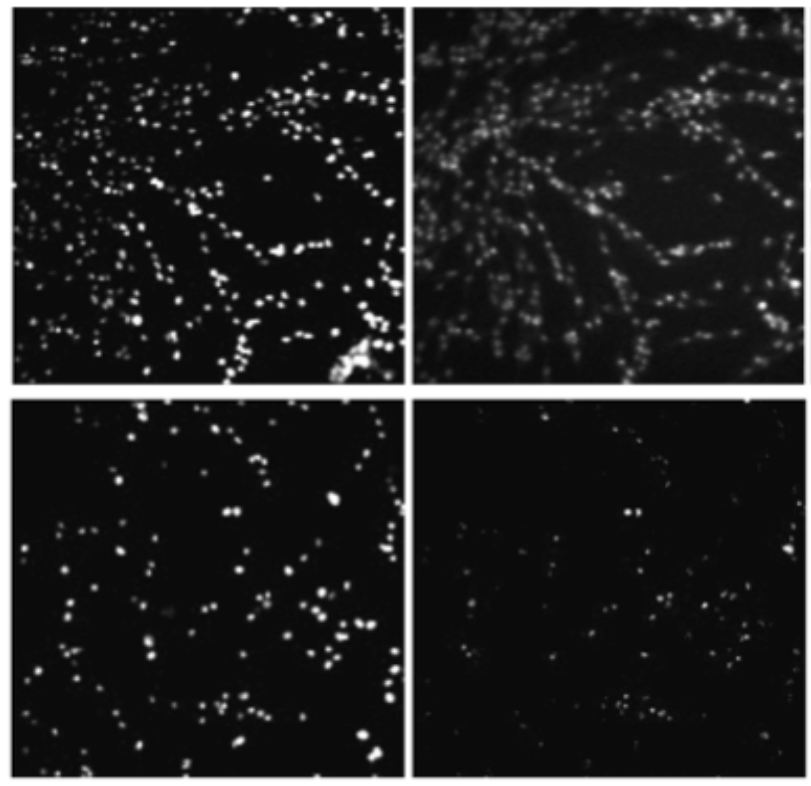

Figure 3

A

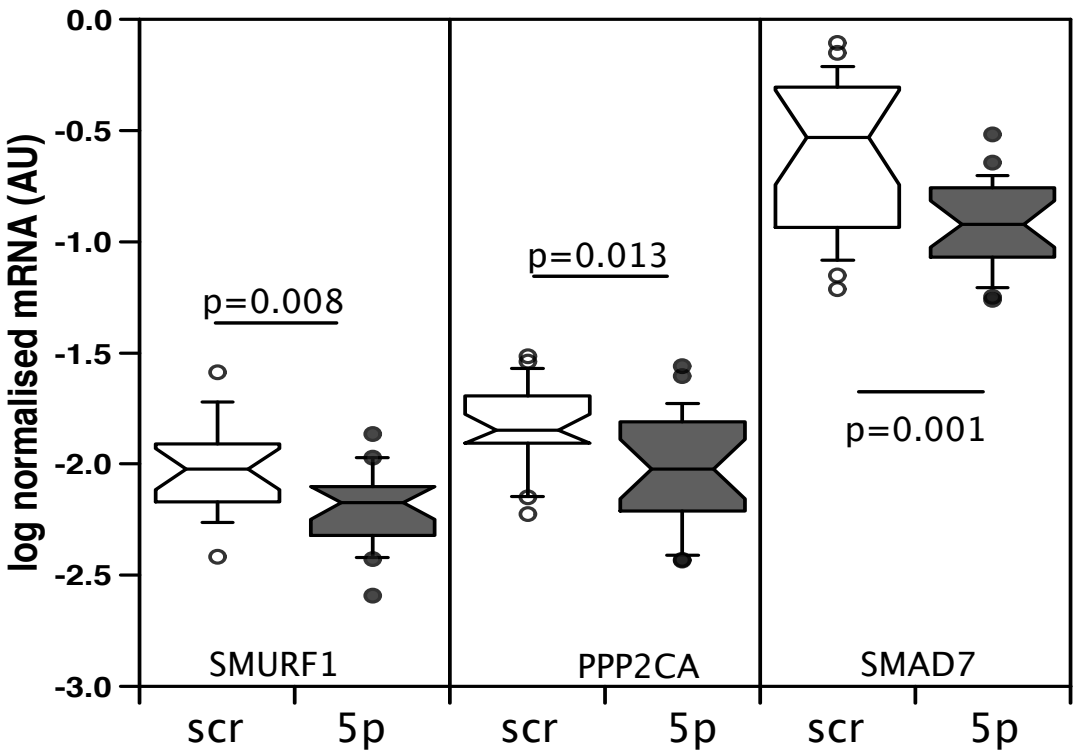

B

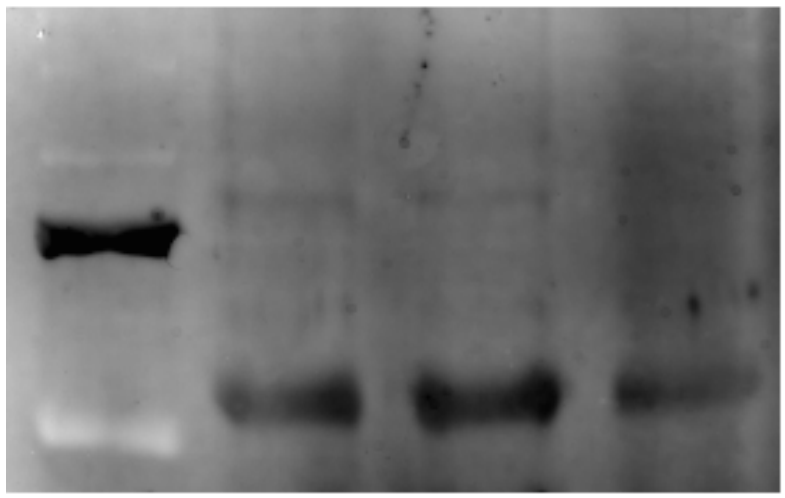

SMAD7

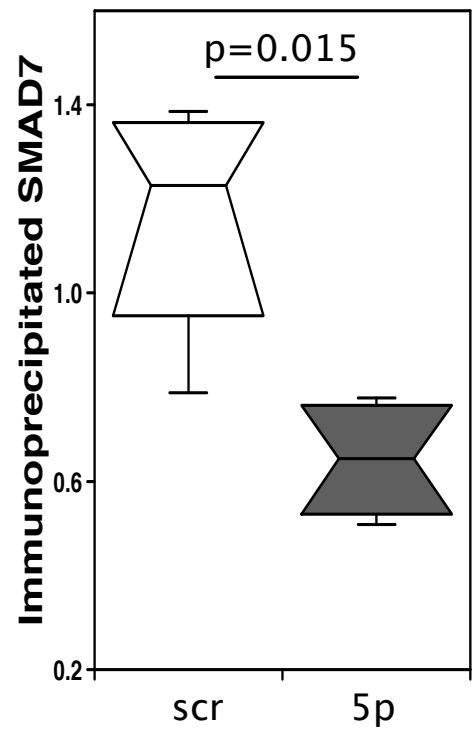

Figure 4

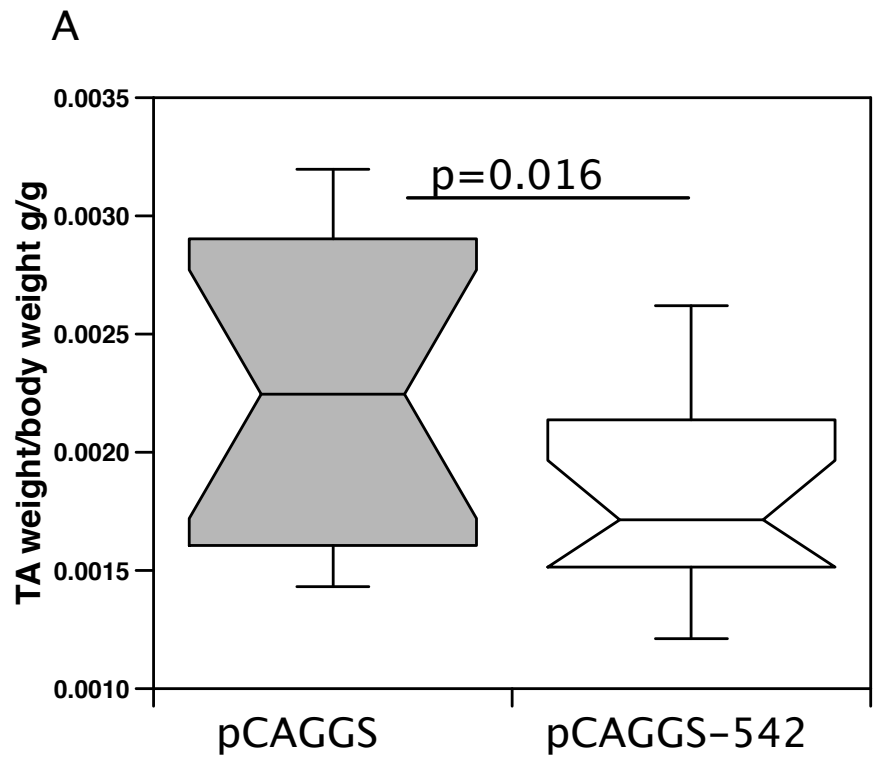
A
TA weight/body weight g/g
0.0035
0.0030
0.0025
0.0020
0.0015
0.0010
p=0.016
pCAGGS
pCAGGS-542

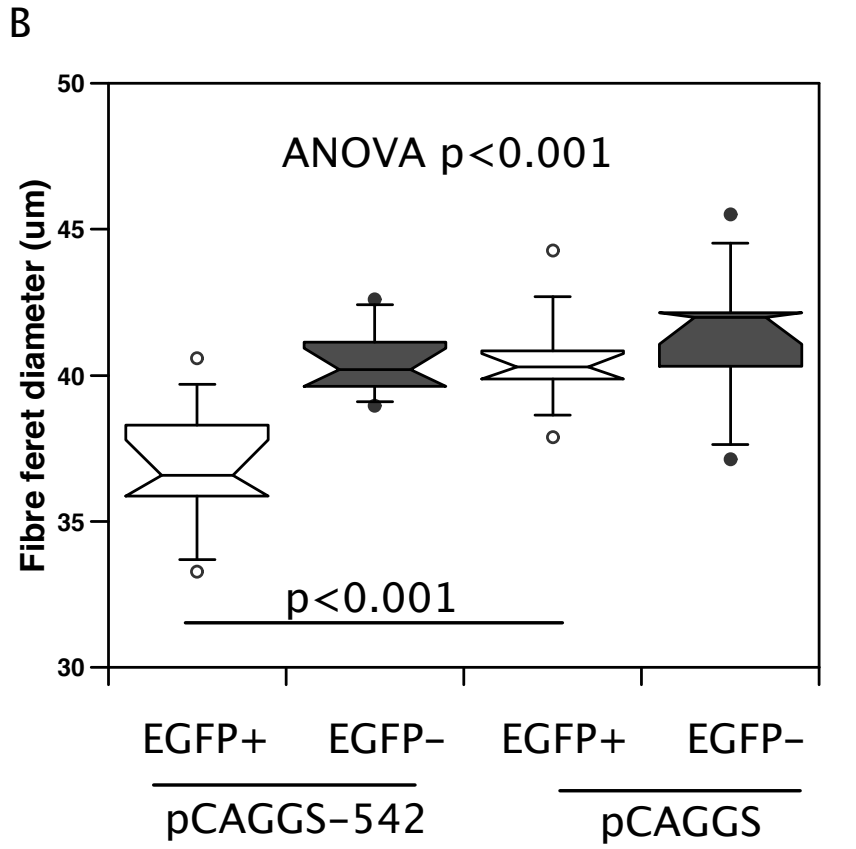
B
Fibre feret diameter (um)
50
45
40
35
30
ANOVA p<0.001
p<0.001
EGFP+
EGFP-
EGFP+
EGFP-
pCAGGS-542
pCAGGS

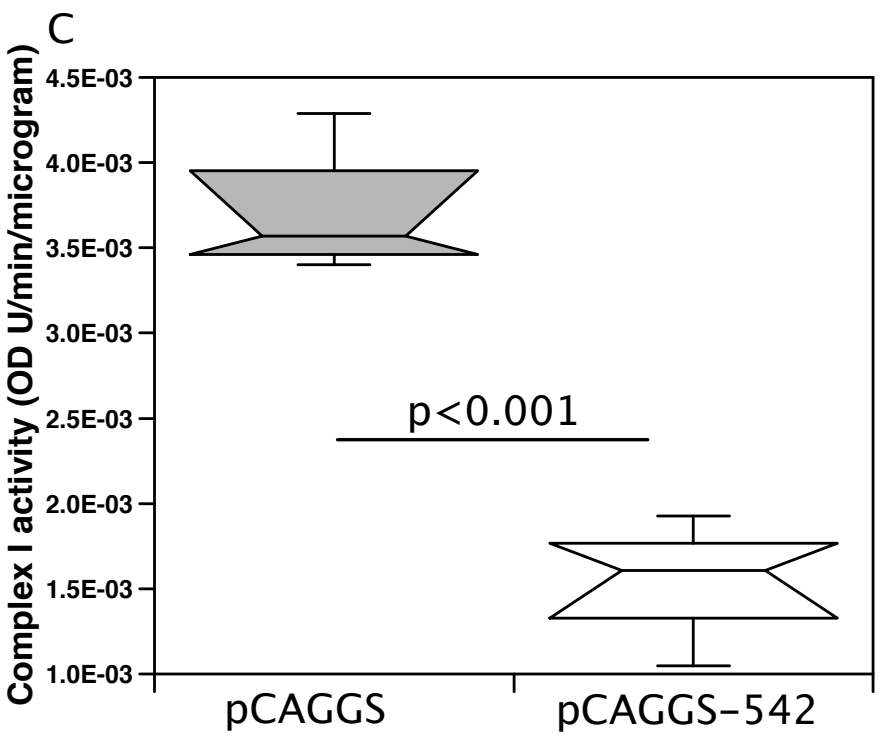
C
Complex I activity (OD U/min/microgram)
4.5E-03
4.0E-03
3.5E-03
3.0E-03
2.5E-03
2.0E-03
1.5E-03
1.0E-03
p<0.001
pCAGGS
pCAGGS-542

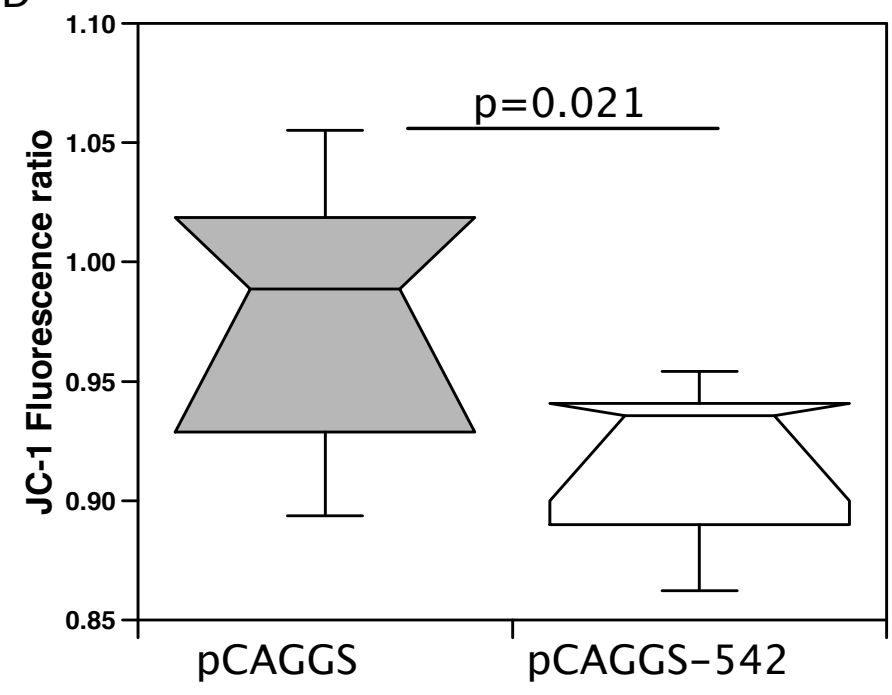
D
JC-1 Fluorescence ratio
1.10
1.05
1.00
0.95
0.90
0.85
p=0.021
pCAGGS
pCAGGS-542

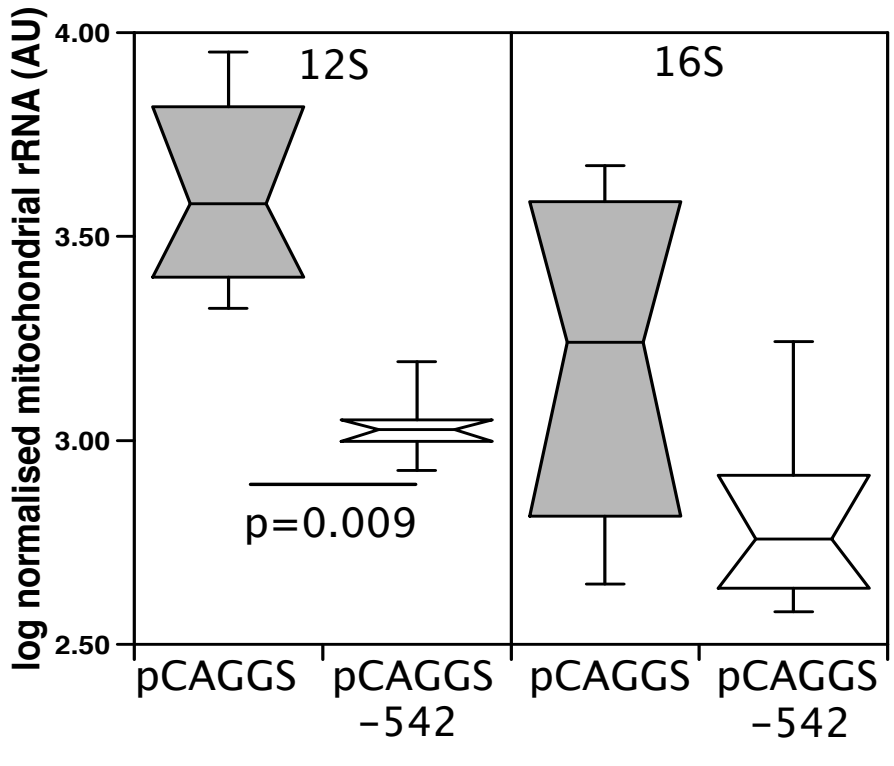
log normalised mitochondrial rRNA (AU)
4.00
3.50
3.00
2.50
12S
16S
p=0.009
pCAGGS
pCAGGS -542
pCAGGS
pCAGGS -542

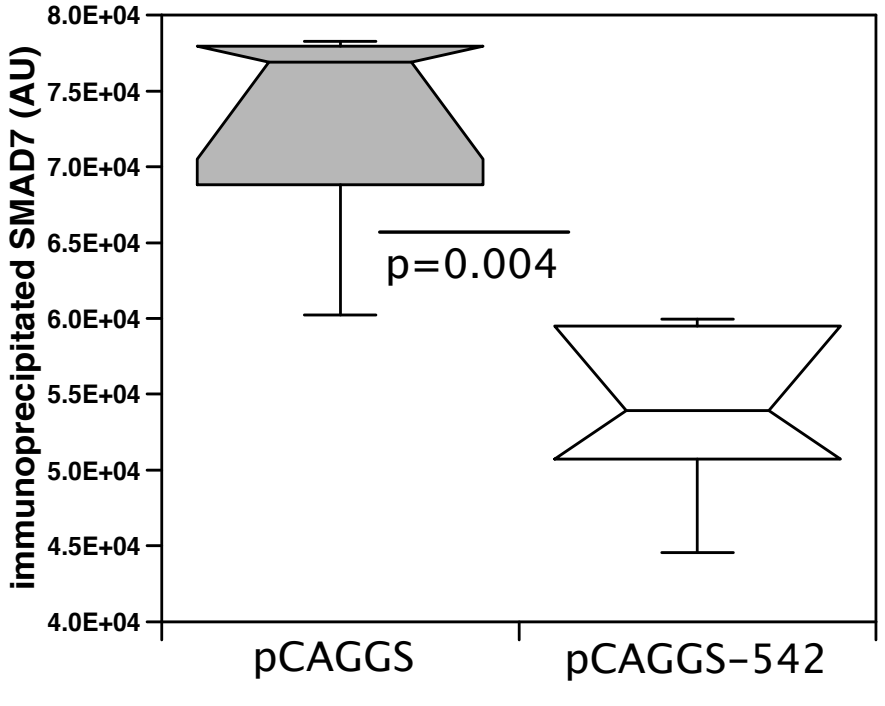
immunoprecipitated SMAD7 (AU)
8.0E+04
7.5E+04
7.0E+04
6.5E+04
6.0E+04
5.5E+04
5.0E+04
4.5E+04
4.0E+04
p=0.004
pCAGGS
pCAGGS-542

Figure 5

A

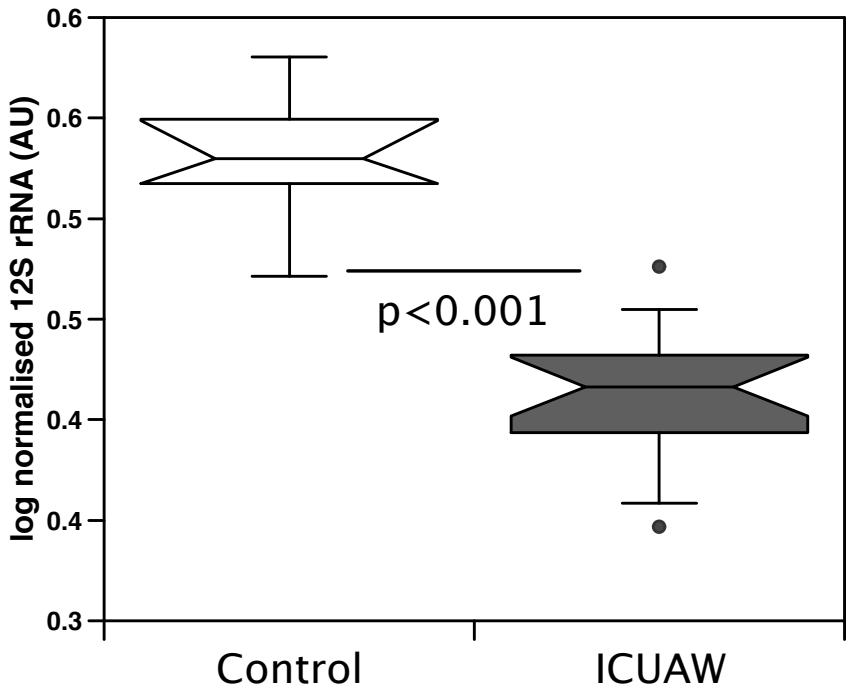
log normalised 12S rRNA (AU)
0.6
0.6
0.5
0.5
0.4
0.4
0.3
p<0.001
Control
ICUAW

B

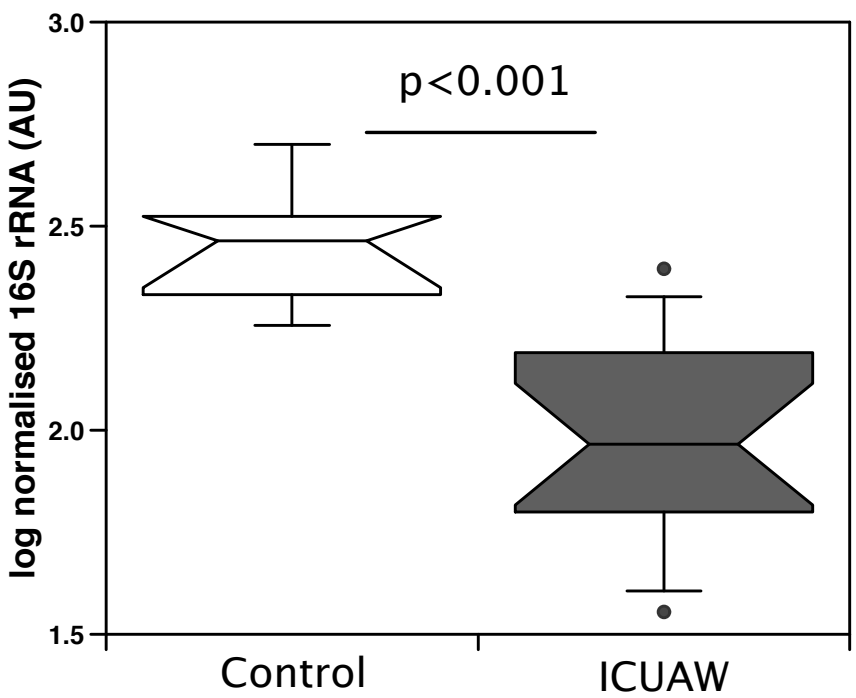
g normalised 16S rRNA (AU)
3.0
2.5
2.0
1.5
p<0.001
Control
ICUAW

C

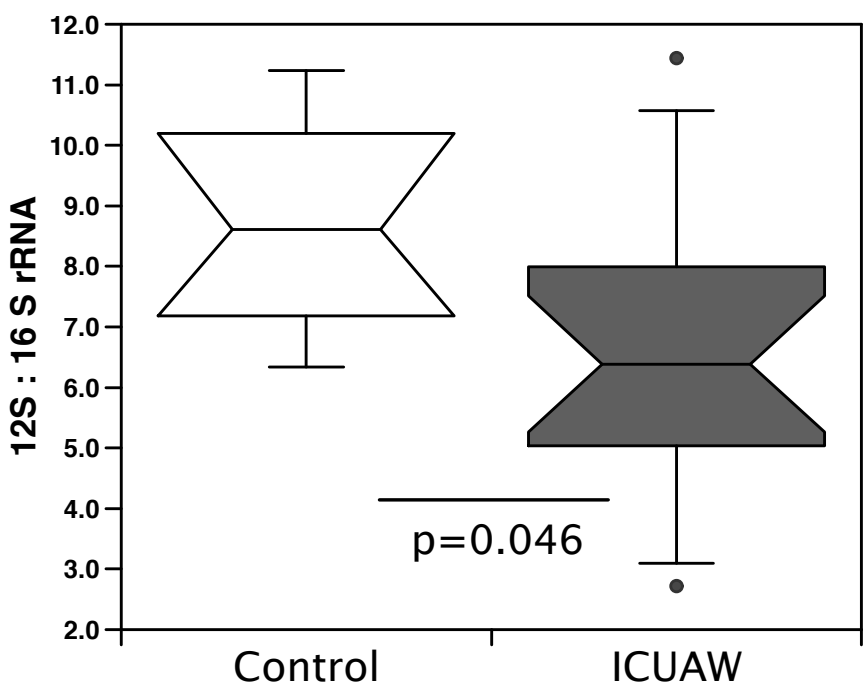
12S : 16 S rRNA
12.0
11.0
10.0
9.0
8.0
7.0
6.0
5.0
4.0
3.0
2.0
p=0.046
Control
ICUAW

Figure 6

A

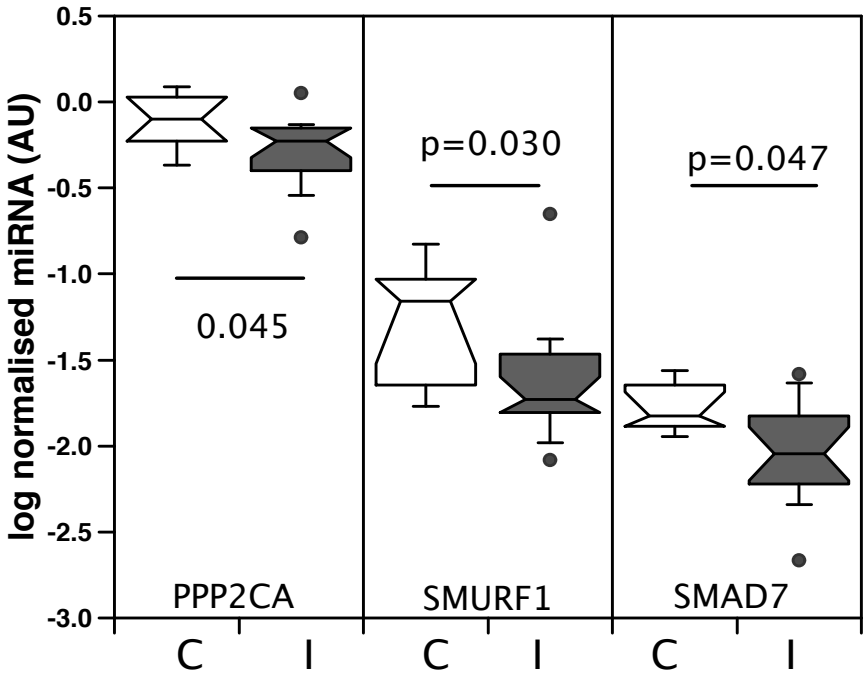
log normalised miRNA (AU)
0.5
0.0
-0.5
-1.0
-1.5
-2.0
-2.5
-3.0
p=0.030
p=0.047
0.045
PPP2CA
SMURF1
SMAD7
C
I
C
I
C
I

B

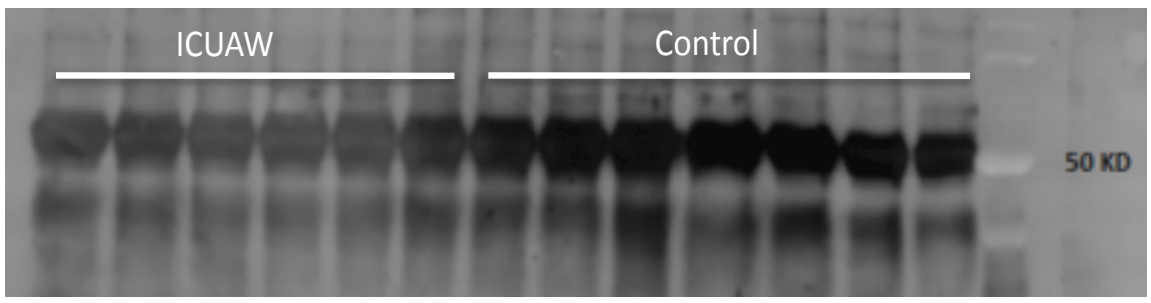
ICUAW
Control
50 KD

C

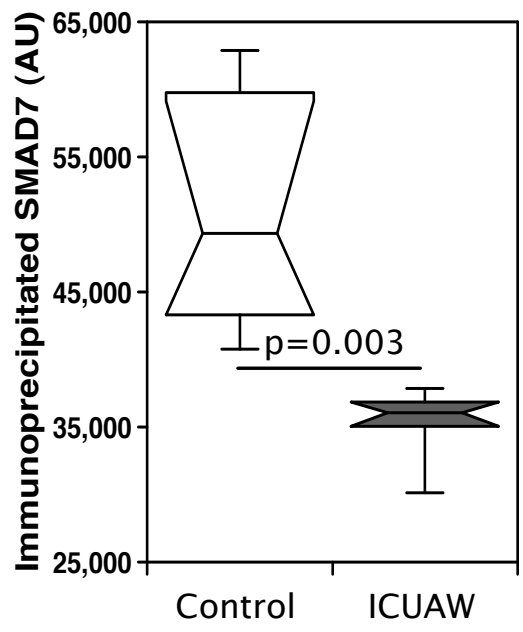
Immunoprecipitated SMAD7 (AU)
65,000
55,000
45,000
35,000
25,000
p=0.003
Control
ICUAW

Figure 7

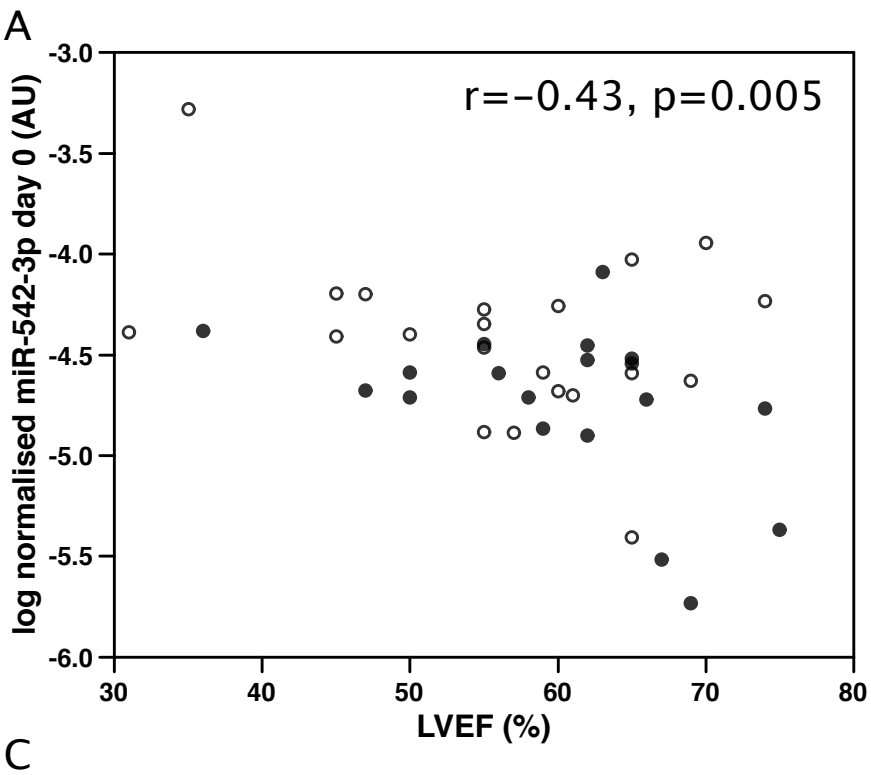
A
r=−0.43, p=0.005
log normalised miR-542-3p day 0 (AU)
LVEF (%)

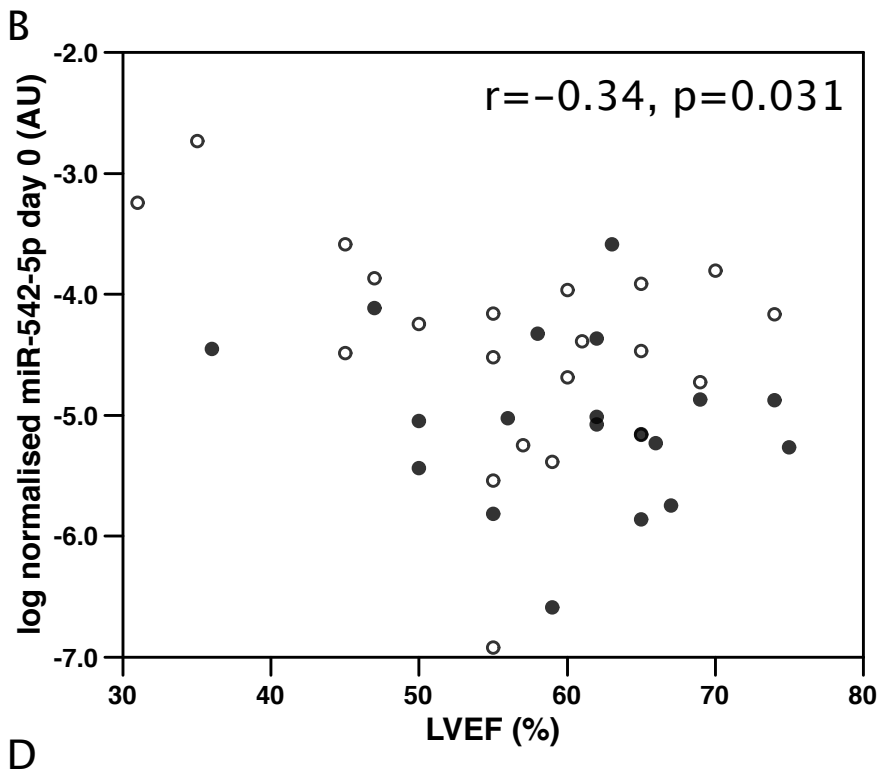
B
r=−0.34, p=0.031
log normalised miR-542-5p day 0 (AU)
LVEF (%)

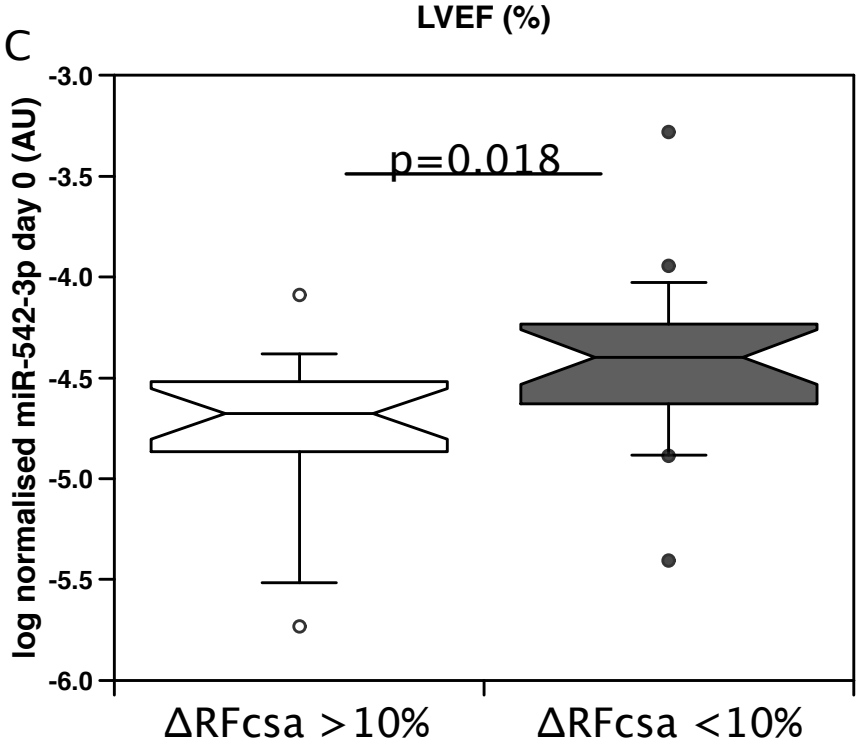
C
p=0.018
log normalised miR-542-3p day 0 (AU)
ΔRFcsa >10%
ΔRFcsa <10%

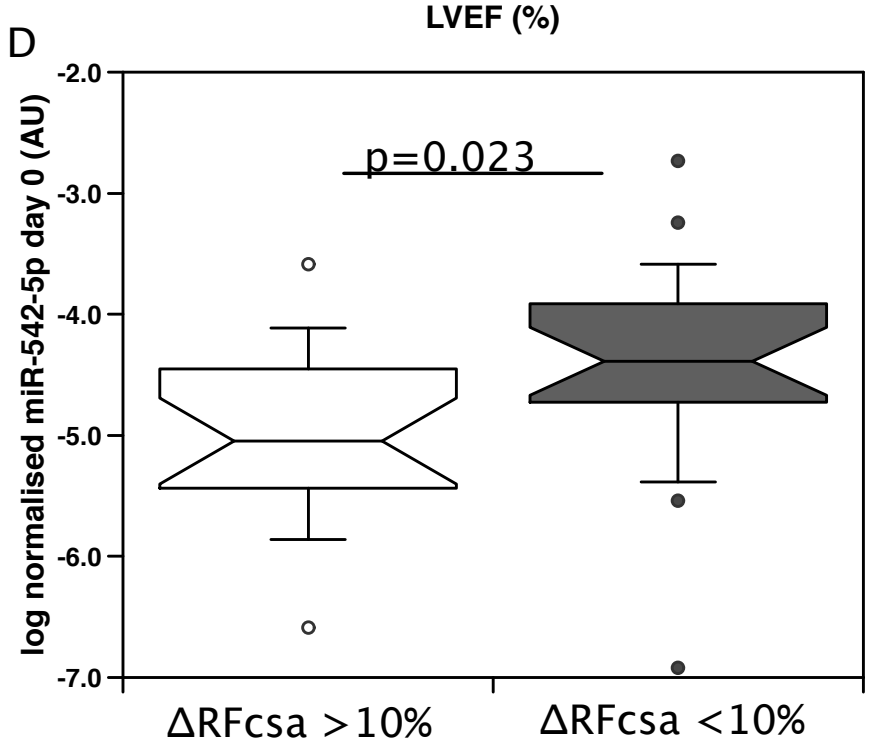
D
p=0.023
log normalised miR-542-5p day 0 (AU)
ΔRFcsa >10%
ΔRFcsa <10%

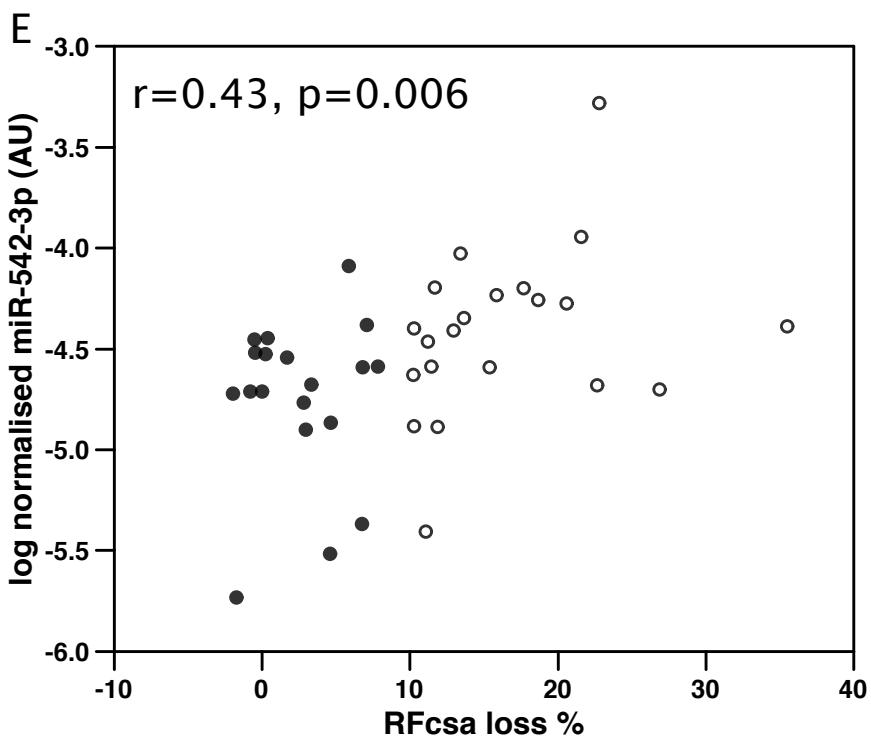
E
r=0.43, p=0.006
log normalised miR-542-3p (AU)
RFcsa loss %

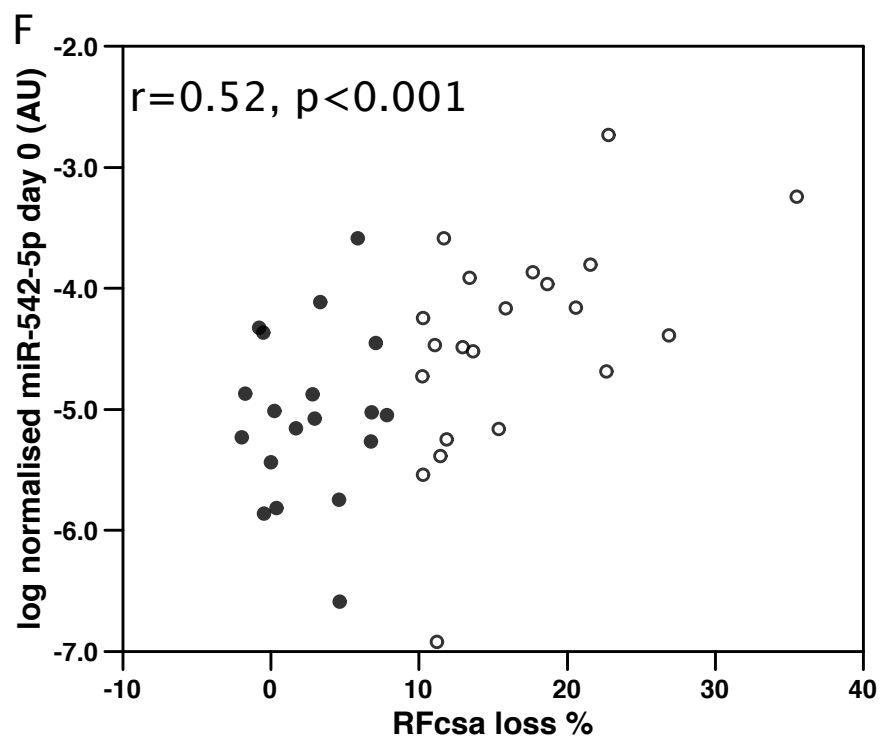
F
r=0.52, p<0.001
log normalised miR-542-5p day 0 (AU)
RFcsa loss %

Figure 8

Table 1. miRNAs differentially expressed in the quadriceps of patients with COPD compared to controls

miRNA	Chromosomal location	mean fold change COPD/cont	p value
hsa-miR-499-5p	20q11.22	0.211	0.006
hsa-miR-144#	17q11.2	0.250	0.006
hsa-miR-367	4q25	0.307	0.005
hsa-miR-302b	4q25	0.335	0.002
hsa-miR-31#	9p21.3	0.344	0.008
hsa-miR-126#	9q34.3	0.359	0.001
hsa-miR-374a#	xq13.2	0.374	0.005
hsa-miR-20a#	13q31.3	0.377	0.005
hsa-miR-651	xp22.31	0.383	0.006
hsa-miR-145#	5q32	0.440	0.006
hsa-miR-31	9p21.3	0.449	0.001
hsa-miR-32	9q31.3	0.456	0.002
hsa-miR-302a	4q25	0.477	0.006
hsa-miR-520c-3p	19q13.42	0.514	0.006
hsa-miR-545	xq13.2	0.530	0.001
hsa-miR-190	15q22.2	0.531	0.005
hsa-miR-598	8p23.1	0.571	0.003
hsa-miR-136#	14q32.31	0.585	0.001
hsa-miR-210	11p15.5	0.604	0.004
hsa-miR-150	19q13.33	0.628	0.008
hsa-miR-576-3p	4q25	0.649	0.008
hsa-miR-340	5q35.3	0.683	0.004
hsa-miR-590-5p	7q11.23	0.702	0.004
hsa-miR-652	xq23	0.723	0.007
hsa-miR-30c	1p34.2, 6q13	0.744	0.004
hsa-miR-140-5p	16q22.1	0.786	0.008
hsa-miR-128	2q21.3, 3p21.3	1.731	0.000
hsa-miR-542-3p	xq26.3	4.073	0.000
hsa-miR-424	xq26.3	4.124	0.000
hsa-miR-450a	xq26.3	4.728	0.000
hsa-miR-424#	xq26.3	6.723	0.004
hsa-miR-542-5p	xq26.3	9.617	0.001

References

1. Man WD, Kemp P, Moxham J, Polkey MI. Skeletal muscle dysfunction in COPD: clinical and laboratory observations. *Clin Sci (Lond)* 2009; 117: 251-264.
2. De Jonghe B, Bastuji-Garin S, Sharshar T, Outin H, Brochard L. Does ICU-acquired paresis lengthen weaning from mechanical ventilation? *Intensive Care Med* 2004; 30: 1117-1121.
3. De Jonghe B, Sharshar T, Lefaucheur JP, Authier FJ, Durand-Zaleski I, Boussarsar M, Cerf C, Renaud E, Mesrati F, Carlet J, Raphael JC, Outin H, Bastuji-Garin S, Groupe de Reflexion et d'Etude des Neuromyopathies en R. Paresis acquired in the intensive care unit: a prospective multicenter study. *JAMA* 2002; 288: 2859-2867.
4. Ali NA, O'Brien JM, Jr., Hoffmann SP, Phillips G, Garland A, Finley JC, Almoosa K, Hejal R, Wolf KM, Lemeshow S, Connors AF, Jr., Marsh CB, Midwest Critical Care C. Acquired weakness, handgrip strength, and mortality in critically ill patients. *Am J Respir Crit Care Med* 2008; 178: 261-268.
5. Fletcher SN, Kennedy DD, Ghosh IR, Misra VP, Kiff K, Coakley JH, Hinds CJ. Persistent neuromuscular and neurophysiologic abnormalities in long-term survivors of prolonged critical illness. *Crit Care Med* 2003; 31: 1012-1016.
6. Swallow EB, Reyes D, Hopkinson NS, Man WD, Porcher R, Cetti EJ, Moore AJ, Moxham J, Polkey MI. Quadriceps strength predicts mortality in patients with moderate to severe Chronic Obstructive Pulmonary Disease. *Thorax* 2007; 62: 115-120.
7. Bloch SA, Lee JY, Syburra T, Rosendahl U, Griffiths MJ, Kemp PR, Polkey MI. Increased expression of GDF-15 may mediate ICU-acquired weakness by down-regulating muscle microRNAs. *Thorax* 2015; 70: 219-228.
8. Bloch SA, Lee JY, Wort SJ, Polkey MI, Kemp PR, Griffiths MJ. Sustained elevation of circulating growth and differentiation factor-15 and a dynamic imbalance in mediators of muscle homeostasis are associated with the development of acute muscle wasting following cardiac surgery. *Crit Care Med* 2013; 41: 982-989.
9. Patel MS, Lee JY, Baz M, Wells CE, Bloch SAA, Lewis A, Donaldson AV, Garfield BE, Hopkinson NS, Natanek SA, Man WD-C, Wells DJ, Baker EH, Polkey MI, Kemp PR. GDF-15 is associated with muscle mass in COPD and promotes muscle wasting in vivo. *J Cachexia Sarcopenia and Muscl* 2016; 7: 436–448.
10. Puig-Vilanova E, Martinez-Llorens J, Ausin P, Roca J, Gea J, Barreiro E. Quadriceps muscle weakness and atrophy are associated with a differential epigenetic profile in advanced COPD. *Clin Sci (Lond)* 2015; 128: 905-921.
11. Brealey D, Brand M, Hargreaves I, Heales S, Land J, Smolenski R, Davies NA, Cooper CE, Singer M. Association between mitochondrial dysfunction and severity and outcome of septic shock. *Lancet* 2002; 360: 219-223.
12. Jiroutkova K, Krajcova A, Ziak J, Fric M, Waldauf P, Dzupa V, Gojda J, Nemcova-Furstova V, Kovar J, Elkalaf M, Trnka J, Duska F. Mitochondrial function in skeletal muscle of patients with protracted critical illness and ICU-acquired weakness. *Crit Care* 2015; 19: 448.
13. van den Borst B, Slot IG, Hellwig VA, Vosse BA, Kelders MC, Barreiro E, Schols AM, Gosker HR. Loss of quadriceps muscle oxidative phenotype and decreased endurance in patients with mild-to-moderate COPD. *J Appl Physiol (1985)* 2013; 114: 1319-1328.
14. Natanek SA, Gosker HR, Slot IG, Marsh GS, Hopkinson NS, Man WD-C, Tal-Singer RM, Moxham J, Kemp PR, Schols AMWJ, Polkey MI. Heterogeneity of Quadriceps Muscle Phenotype in Chronic Obstructive Pulmonary Disease (COPD); Implications for Stratified Medicine? *Muscle and Nerve* 2013; 48: 488-497.
15. Chen JF, Mandel EM, Thomson JM, Wu Q, Callis TE, Hammond SM, Conlon FL, Wang DZ. The role of microRNA-1 and microRNA-133 in skeletal muscle proliferation and differentiation. *Nat Genet* 2006; 38: 228-233.

16. Zhang X, Zuo X, Yang B, Li Z, Xue Y, Zhou Y, Huang J, Zhao X, Zhou J, Yan Y, Zhang H, Guo P, Sun H, Guo L, Zhang Y, Fu XD. MicroRNA directly enhances mitochondrial translation during muscle differentiation. *Cell* 2014; 158: 607-619.
17. Lewis A, Riddoch-Contreras J, Natanek SA, Donaldson A, Man WD, Moxham J, Hopkinson NS, Polkey MI, Kemp PR. Downregulation of the serum response factor/miR-1 axis in the quadriceps of patients with COPD. *Thorax* 2012; 67: 26-34.
18. Watson E, Sylvius NB, Viana JLL, Greening N, Barratt J, Smith A. Differential MicroRNA Expression In Skeletal Muscle Of Human CKD Patients And Healthy Controls. *Nephrology Dialysis Transplantation* 2016; 31 (Supplement): i472–i478.
19. Lewis A, J.Y. L, Donaldson AV, Natanek AS, Vaidyanathan S, Man WD, Hopkinson NS, Sayer AA, Patel HP, Cooper C, Syddall H, Polkey MI, Kemp PR. Increased expression of H19/miR-675 is associated with a low fat-free mass index in patients with COPD. *J Cachexia Sarcopenia and Muscle* 2016; 7:330-334.
20. Farre-Garros R, Natanek SA, Bloch S, Polkey MI, Kemp PR. miR-542: a novel regulator of muscle mass and function. *J Muscle Res Cell Motil* 2015; 36: 593-594.
21. Farre-Garros R, Paul R, Natanek SA, Griffiths M, Polkey MI, Kemp PR. A microRNA axis that regulates muscle mass and mitochondrial function in response to disease. *J Muscle Res Cell Motil* 2017: S08.O05-253.
22. Paul R, Polkey M, Kemp P, Griffiths M. S116 GDF-15, the miR-542 cluster and miR-422a are associated with muscle wasting in Intensive Care Unit Acquired Paresis. *Thorax* 2015; 70: A66-A67.
23. Rabe KF, Hurd S, Anzueto A, Barnes PJ, Buist SA, Calverley P, Fukuchi Y, Jenkins C, Rodriguez-Roisin R, van WC, Zielinski J. Global strategy for the diagnosis, management, and prevention of chronic obstructive pulmonary disease: GOLD executive summary. *AmJRespirCrit Care Med* 2007; 176: 532-555.
24. Bergstrom J. Percutaneous needle biopsy of skeletal muscle in physiological and clinical research. *Scand J Clin Lab Invest* 1975; 35: 609-616.
25. Seymour JM, Ward K, Sidhu PS, Puthucheary Z, Steier J, Jolley CJ, Rafferty G, Polkey MI, Moxham J. Ultrasound measurement of rectus femoris cross-sectional area and the relationship with quadriceps strength in COPD. *Thorax* 2009; 64: 418-423.
26. Dweep H, Sticht C, Pandey P, Gretz N. miRWalk--database: prediction of possible miRNA binding sites by "walking" the genes of three genomes. *J Biomed Inform* 2011; 44: 839-847.
27. Wang Y, Huang JW, Castella M, Huntsman DG, Taniguchi T. p53 is positively regulated by miR-542-3p. *Cancer Res* 2014; 74: 3218-3227.
28. Yan X, Liu Z, Chen Y. Regulation of TGF-beta signaling by Smad7. *Acta Biochim Biophys Sin (Shanghai)* 2009; 41: 263-272.
29. Dennler S, Itoh S, Vivien D, ten Dijke P, Huet S, Gauthier JM. Direct binding of Smad3 and Smad4 to critical TGF beta-inducible elements in the promoter of human plasminogen activator inhibitor-type 1 gene. *Embo J* 1998; 17: 3091-3100.
30. Bloch S, Polkey MI, Griffiths M, Kemp P. Molecular mechanisms of intensive care unit-acquired weakness. *Eur Respir J* 2012; 39: 1000-1011.
31. Jiroutkova K, Krajcova A, Ziak J, Fric M, Waldauf P, Dzupa V, Gojda J, Nemcova-Furstova V, Kovar J, Elkalaf M, Trnka J, Duska F. Mitochondrial function in skeletal muscle of patients with protracted critical illness and ICU-acquired weakness. *Crit Care* 2015; 19: 448.
32. Brealey D, Singer M. Mitochondrial Dysfunction in Sepsis. *Curr Infect Dis Rep* 2003; 5: 365-371.
33. Saada A, Shaag A, Arnon S, Dolfin T, Miller C, Fuchs-Telem D, Lombes A, Elpeleg O. Antenatal mitochondrial disease caused by mitochondrial ribosomal protein (MRPS22) mutation. *J Med Genet* 2007; 44: 784-786.
34. Miller C, Saada A, Shaul N, Shabtai N, Ben-Shalom E, Shaag A, Hershkovitz E, Elpeleg O. Defective mitochondrial translation caused by a ribosomal protein (MRPS16) mutation. *Ann Neurol* 2004; 56: 734-738.

35. Fredriksson K, Tjader I, Keller P, Petrovic N, Ahlman B, Scheele C, Wernerman J, Timmons JA, Rooyackers O. Dysregulation of mitochondrial dynamics and the muscle transcriptome in ICU patients suffering from sepsis induced multiple organ failure. *PLoS One* 2008; 3: e3686.
36. Li Y, Li W, Ying Z, Tian H, Zhu X, Li J, Li M. Metastatic heterogeneity of breast cancer cells is associated with expression of a heterogeneous TGFbeta-activating miR424-503 gene cluster. *Cancer Res* 2014; 74: 6107-6118.
37. Faraonio R, Salerno P, Passaro F, Sedia C, Iaccio A, Bellelli R, Nappi TC, Comegna M, Romano S, Salvatore G, Santoro M, Cimino F. A set of miRNAs participates in the cellular senescence program in human diploid fibroblasts. *Cell Death Differ* 2012; 19: 713-721.
38. Lee JY, Lori D, Wells DJ, Kemp PR. Expression of FHL1 increases myostatin dependent skeletal muscle atrophy. *FEBS Open Bio* 2015;5:753-62.

Supplementary information

Supplementary Methods

Subjects

COPD cohort: COPD subjects in this study form part of a larger well-phenotyped cohort described by Natanek et al (1). Patients with COPD according to the Global Initiative in Obstructive Lung Disease (GOLD) guidelines 2004 (2) were enrolled from clinics at the Royal Brompton Hospital. Patients with a diagnosis of heart, renal or liver failure, a systemic inflammatory or metabolic disorder or a moderate/severe exacerbation (i.e. requiring antibiotics, oral steroids, or hospitalisation) in the preceding 4 weeks were excluded. Healthy age-matched controls were recruited by advertisement. All subjects gave written informed consent and the protocol was approved by the Royal Brompton & Harefield NHS Trust Research Ethics Committee (Studies 06/Q0404/35 and 06/Q0410/54). 14 patients and 7 controls were used in the screen cohort and a separate 24 patients and 12 controls were used in the validation cohort. All individuals studied in these groups were male and all of the patients had severe (GOLD3-4) COPD. Demographic data for the screen and validation cohorts are shown in Supplemental Tables 1 and 2.

Physiological measurements: Measurements of lung volume, using plethysmography, carbon monoxide transfer factor, using the single breath technique (CompactLab, Jaeger, Germany) and post-bronchodilator spirometry were performed according to ATS/ERS guidelines (3). Blood gas tensions were measured in arterialised capillary earlobe blood. Fat-free mass index (FFMI) was calculated using bioelectrical impedance (Bodystat 1500, Bodystat, UK) measured in patients after resting supine for 10 min as described previously (4).

Quadriceps strength was determined by measuring supine isometric maximal voluntary contraction (MVC) as described previously (4) and exercise capacity measured as 6 minute walk distance (6MW) 5 minutes after bronchodilator treatment (ATS 2002 guidelines (5)) as described previously (1). Muscle biopsy was performed by percutaneous needle biopsy of the *vastus lateralis* in the mid-thigh of the leg in which strength was tested under local anaesthesia using the Bergstrom technique (6).

Intensive Care unit acquired weakness (ICUAW) cohort: This cohort has been described previously (7). Written informed consent was obtained from study subjects or their next of kin and the study was approved by the National Research Ethics Committee (study 10/H0722/9). The principal inclusion criteria was a physician diagnosis of ICUAW using standard diagnostic criteria. MRC strength scoring was included in this diagnosis where the patient was able to co-operate (n=8) but where they were unable to do so, unexplained muscle wasting and weakness according to Stephen's criteria were required. All patients had been admitted to the cardiothoracic ICU at the Royal Brompton Hospital for more than 1 week. The controls for this study were patients undergoing elective cardiothoracic surgery with an MRC score of 60/60. The muscle biopsies were taken from the *rectus femoris* by the Bergstrom technique (6) or as open biopsies. Controls were biopsied prior to surgery.

Aortic surgery cohort: Patients provided written informed consent and the study was approved by the National Research Ethics Committee (study 13/LO/0479). Patients undergoing elective cardiothoracic surgery at Royal Brompton Hospital were recruited. The principal inclusion criterion was a high risk elective aortic surgical procedure requiring admission to the ICU as advised by the surgical team. Pre-surgical exclusion criteria included pre-existing muscular or neuromuscular disease, malignancy, contraindication to muscle

biopsy. Patients were also excluded if they were unstable after surgery or unable to have a post-surgery biopsy. The cross sectional areal of the *rectus femoris* was determined by ultra-sound prior to surgery and 7 days after surgery, as previously described (8). An open biopsy after the induction of anaesthesia but before the start of surgery from the *rectus femoris* and a second biopsy was taken by the Bergstrom technique 24h after surgery. Blood samples were collected prior to surgery and regularly during the first 7 days after surgery. Demographic data for these patients are shown in Supplemental Table 3.

***Assessment of miRNA levels*:** Total RNA was extracted and quantified by quantitative real time PCR (qRTPCR) as described previously (9). MicroRNA expression was analysed in Trizol extracted RNA. RNA isolated muscle was reverse transcribed using MultiScribe™ Reverse Transcriptase with, Megaplex™ RT Primers (human pools A and B, Version 3.0, Applied Biosystems) according to the manufacturer's instructions. The reactions were terminated by heating to 85°C for 5min and the cDNA stored at -80°C. The cDNAs were pre-amplified using Megaplex™ PreAmp Primers (Applied Biosystems) for 12 cycles of 95°C for 15 sec and 60°C for 4 min. The reaction was terminated by heating to 99.9°C for 10 min and pre-amplified cDNA diluted by addition of 75µl of 0.1× TE buffer pH 8.0 (Qiagen) and stored at -80°C.

Quantification of single microRNAs using TaqMan® probes: For the quantification of individual microRNAs, custom designed primers and probes were purchased for each test gene from Applied Biosystems and amplification was carried out on cDNA pre-amplified as described above according to the manufacturer's instructions. Each reaction was performed in duplicate and the average Ct value normalised to the corresponding geometric mean of U6 and RNU48 using the ΔΔ Ct method. RNA isolated from cells was analysed using single RT reactions.

Quantification of mRNA and rRNA: Messenger RNA and ribosomal RNA were extracted and quantified by quantitative real time PCR (qRTPCR) as described previously (9) using primers shown in Table S4. All mRNA and rRNA data was normalized to the geometric mean of the values for beta-2 microglobulin and HPRT.

Cell culture: LHCN-M2 cells were maintained in skeletal muscle growth medium (PromoCell) supplemented with 20% FCS. RNA was extracted using Trizol; mRNA and miRNAs were quantified as described above.

Ago2 pull-down assay

LHCN-M2 cells were cultured in 10cm culture dishes and transfected with either miR-542-5p mimic, miR-542-3p mimic or control mimic and cultured for a further 2 days. The cells were washed twice with ice-cold PBS then lysed with cell lysis buffer (CLB, Promega) supplemented with protease inhibitor cocktail (Sigma). Each lysate was pre-cleared (G-sepharose beads for 2h at 4°C) then divided into 2. Ago2 and bound RNAs were immunoprecipitated by incubation of the lysate in 1x CLB, G-sepharose beads [prepared by pre-incubation in CLB supplemented with salmon sperm DNA (0.2mg/ml) and BSA (1mg/ml)] with either anti-ago2 antibody (Millipore, Billerica, MA., USA) or anti-IgG antibody, overnight at 4^{o}C under rotation. The beads were washed in CLB, x1, IP buffer (50mM Tris (pH 7.4), 5mM $MgCl_2$, 300mM NaCl, 0.05% NP40) x4, and PBS x1. RNA was extracted from the beads using TRIzol and cDNA synthesised. Data for each cDNA were normalised to the geometric mean of RPLPO, 12S rRNA and 16S rRNA in the same sample and analysed as fold enrichment (anti-Ago2/control IgG) compared to control mimic transfection.

Immunofluorescence analysis: After treatment, the myoblasts were washed twice with 1xPBS then fixed with 4% PFA followed by 2 washes with 1xPBS supplemented with

Tween20 (0.05%, PBS-0.05T). Cells were incubated in PBS supplemented with 0.3% Triton for 15 minutes at RT and washed twice with 1x PBS-0.05T. After 1 hour incubation in 1x PBS-0.05T supplemented with 5% BSA (w/v) blocking solution, the primary antibody in PBS-0.05T supplemented with 5% BSA was added to cells for 1 hour at RT. The cells were washed 3 times with 1xPBS-0.05T then incubated with secondary antibody in 1x PBS-0.05T supplemented with 5% BSA for 1 hour at RT. The cells were then incubated in 1xPBS-0.05T supplemented with DAPI (1:10000) to stain nuclei, then washed a final two times in 1xPBS-0.05T. Cells were imaged on a Zeiss Axiovert widefield microscope and data collected and analysed using Volocity software.

Immunoprecipitation and Western blotting

Immunoprecipitation: 5μg of muscle homogenate or 60 μl of cell homogenate were incubated with 5μl of rabbit anti-SMAD7 antibody (H-79, Santa Cruz) in a total volume of 400μl for 1h at 4°C before 20μl of protein A beads were added and the samples incubated overnight. The beads were collected by centrifugation 2500 rpm in a microcentrifuge for 5 min at 4°C and the immunoprecipitates were washed 4 times with PBS. The pelleted beads were then used as the protein sample.

Western Blot analysis: Protein samples were boiled in sample buffer TRIS (62.5mM) pH 6.8, Glycerol (25%), SDS (2%), Bromophenol-blue (0.01%), β-Mercaptoethanol (1:20) for 5mins prior to SDS PAGE. The proteins were separated at 135V (252mA) on 10% acrylamide gels before being transferred PVDF membranes. The membranes were blocked with milk (5%) and Tween-20 (0.1%) in TBS for 1hr at room temperature. The blots were incubated in primary antibody [goat anti-SMAD7 (P20, Santa Cruz), rabbit anti-MRPS10 (Pierce), rabbit anti-CytB (Pierce), rabbit anti pSMAD2/3 (cell signaling) or rabbit anti SMAD2/3 (Santa Cruz)]

made up in PBS with Tween-20 (0.1%) supplemented with dry milk powder (5% w/v) overnight at 4ºC. The following day the membranes were washed three times for 5 mins in PBS-0.1T and incubated for 1h with the appropriate horseradish peroxidase-conjugated secondary antibody diluted 1:3000 in PBS-0.1T supplemented with 5% (w/v) dried milk powder. The membranes were subsequently washed three times for 5 mins in TBS + Tween-20 (0.1%). The blot was visualised with a chemiluminescent detection reagent kit (Amersham ECL reagent cat no: RPN 2106).

In vitro experiments

Cell culture: Human skeletal myoblasts cells, LHCN-M2, were grown in skeletal muscle growth media supplemented with 20% (v/v) fetal bovine serum (FBS) at 37°C in humidified 5% CO_2, 95% atmospheric air. Cells were not allowed to exceed 70% confluence, so cells were subcultured by trypsinisation (1:4 for LHCN-M2).

MicroRNA transfection: Cells were seeded at a density of $5x10^4$ cells/mL, (seeding 6250 cells in a 96-well plate well and scaling it for appropriate growth area). After 24 hours, cells were transfected with mirVana miRNA mimics, using Lipofectamine 2000 according to the manufacturer's instructions.

RNA extraction: 48h after microRNA transfection, RNA was extracted from LHCN-M2 cells in a 96-well plate using the CellAmp Direct RNA Prep Kit (TaKaRa) according to the manufacturer's instructions.

Luciferase Assays: Cells were seeded at a density of $5x10^4$ cells/mL, seeding in a 96-well plate well 6250 cells and scaling it for appropriate growth area. After 24 hours, cells were transfected with mirVana miRNA mimics, using Lipofectamine 2000 (Thermo Fischer)

according to the manufacturer's instructions. 24 hours after transfection with mirVana miRNA mimic, cells were transfected with luciferase reporter vectors: according to the manufacturer's instructions. In each well of a 96-well plate, 0.094 µg of vector-Luc and 0.031 µg of pRLTK construct were used. Cells were allowed to recover overnight in complete medium before being washed twice with serum free DMEM, and addition of TGF-β for 2h or 6h. Cells were lysed and assayed using the DualGlo Luciferase Assay Kit (Promega) according to the manufacturer's instructions and firefly luciferase values to normalized to Renilla Luciferase values. Experiments were conducted in sextuplets and repeated twice.

Membrane potential analysis: Mitotracker Red (Thermo Fischer): 48h after microRNA transfection, 250 nM Mitotracker red in skeletal muscle media was added in each well and incubated for 15 min at room temperature. Cells were washed with PBS twice and fixed with PFA and DAPI nucleus staining was carried out. JC-1 staining (Thermo Fischer): 48h after microRNA transfection, cells were incubated with 10 µM JC-1 in skeletal muscle for 10 min at 37˚C. Cells were washed twice with PBS and intensities were measured at paired excitation and emission wavelengths of 485/530 (green) and 530/590 (red) with a CYTOFLUOR *(Applied Biosystems)* plate reader.

DNA extraction: 48h after microRNA transfection, cells were washed with PBS and incubated with 800 µL of lysis buffer (200mM Tris/HCl pH 7.5, 25 mM EDTA pH 8, 250 mM NaCl, 0.5% SDS) for 1h at 37˚C. Lysed cells were transferred to an Eppendorf tube and 10mg/mL of proteinase K solution and 10 µg/mL RNAse A were added and incubated at 50˚C for 1h. 280 µL of saturated NaCl were added to the mix and vortexed for 5 min then centrifuged at 13000 rpm for 10 min. The DNA was precipitated from the supernatant by adding 600µL of isopropanol. Following centrifugation the pellet was washed with 1mL of 70% ethanol and resuspended in 120 µL of 1X TE.

In vivo experiments

Cloning of expression vector for miR-542. A 500 bp fragment of the miR-542 locus was amplified from genomic DNA by PCR using the primers GGGAGATCTCTCTGGTGGCTGAAAGTAGAG and GGGAGATCTCTAGGCTTCAGTGGACTGAATAG. The PCR product was cloned into pGEM-T-easy, sequenced then shuttled into the BamHI site of pCAGGS-EGFP and the orientation confirmed.

Electroporation: Mouse experiments were approved by the Imperial College Ethical Review Process and were licensed by the UK Secretary of State for the Home Office under Project License PPL 70/8297. Five male C57/Bl6 mice (7.5 weeks old) were anaesthetised with Hypnorm (VetaPharma) and Hypnovel (Roche), both lower legs were shaved and 10U (25μl) of bovine hyaluronidase (Sigma) was injected into each TA (10, 11). Mice were allowed to partially recover at 37^{o}C and after 2 hours were re-anaesthetised using 5% isofluorane then maintained at 2% isofluorane. The TA muscles were injected with 25μl of the appropriate plasmid at 1μg/μL before electro-conductive cream was applied to electrodes which were placed either side of TA, separated by approximately 5mm. Electroporation was performed using 10 pulses of 85V each for 20 msec, at a frequency of 1 Hz. This experiment was repeated 3 times. In each experiment mean TA weight normalized for bodyweight was lower in the pCAGGS-miR-542 group than in the pCAGGS alone group and in two of the 3 experiments this reduction reached statistical significance (paired tTest).

Following electroporation, mice recovered and were left for 3 days prior to sacrifice. The TA muscle was removed and weighed before either being embedded (2 sets of mice) or fractionated into mitochondrial, nuclear and cytoplasmic fractions using the mitochondrial

isolation kit (Thermo Scientific) (one set of mice). Protein was quantified by Bradford assay. Mitochondrial membrane potential was determined using 20μg of mitochondrial protein in a standard JC-1 assay as described above. Complex I activity was determined on 5μg of mitochondrial protein in a complex I assay (Abcam) according to the manufacturer's instructions. SMAD7 was immunoprecipitated from the cytoplasmic fraction.

Laser capture microdissection was performed on samples embedded in OCT and sectioned onto PEN membrane. EGFP fluorescent areas of the muscle were identified and isolated using a PALM LCM system (Zeiss). RNA was harvested using the microRNEasy (Qiagen).

Statistical analysis: Gene expression data were log transformed to produce normal distribution and stabilise variance. Person correlations were performed for correlation analysis assuming linearity *(Aabel).* Differences between groups were calculated using Student's t-test for normally distributed data or by Mann-Whitney U test for non-parametric data *(Aabel)*. *In vitro* data shown were produced in independent three independent experiments, for gene expression data and luciferase assays treatments were performed in sextuplet within each experiment.

Supplementary Results and Discussion

TGF-β signalling and miR-542-5p

Targets for miR-542-5p were identified using miRwalk 2.0 to identify mRNAs that were predicted by at least 3 different algorithms (12). Amongst the human targets were SMAD3, SMAD6, SMAD7, Alk5, TGFBR2, TGFBR3, SMURF1 and protein phosphatases involved in the dephosphorylation of SMAD2/3, PPM1A, CTDSP1, CTDSP2 and components of the PP2A complex; PPP2CA, PPP2R2C, PPP2R2D and PPP2R5A. These proteins are all components of the TGF-β signalling pathway (Fig S3) and suggested that this pathway may be modulated by

miR-542-5p. Consistent with this suggestion miR-542-5p increased basal luciferase from a SMAD dependent reporter gene as shown in Fig. 7A.

Muscle wasting in patients about to undergo aortic surgery

We have previously shown that approximately 50% of patients undergoing aortic surgery will lose more than 10% of their muscle mass over the following 7 days (13). We therefore repeated this study to determine whether we could identify miRNA expression patterns associated with the likelihood of losing muscle. 40 patients were recruited to the study as described in Methods. Clinical parameters for these patients are given in Supplemental Table 4. Ultrasound analysis of the *rectus femoris* prior to surgery and 7 days later showed that 19 patients lost more than 10% of the cross sectional area of this muscle following surgery, consistent with our previous observations. This loss of muscle mass was weakly associated with age ($r=0.33$, $p=0.039$), LVEF% ($r=-0.34$, $p=0.030$, Fig. S2) but not with cross clamp time.

Supplementary figure legends

Figure S1. miR-542-3p is elevated in males with COPD compared to healthy male controls

miR-542-3p was quantified in quadriceps biopsies from COPD patients (n=24) and healthy age-matched controls (n=12). Box and whiskers plot showing that the expression of miR-542-3p was elevated 2 fold in the patients compared to controls (p=0.012 t-test)

Figure S2. miR-542-3p binds to MRPS mRNAs and suppresses Mitotracker Red uptake in LHCN-M2 cells

A. RNA was immunoprecipitated from cells transfected with miR-542-3p mimic or control mimic using anti-Ago2 as described in Supplementary Methods. Levels of MRPS10, S18C, S2 and S27 were quantified by PCR and are presented as fold enrichment in the 542-3p transfected cells normalised to control transfected cells.

B. LHCN-M2 cells were transfected with scrambled miRmimic, miR-542-3p mimic or miR-542-3p mimic in the presence of the antagomiR-542-3p. 48h after transfected the cells were stained with Mitotracker Red, fixed and stained with DAPI then analysed by fluorescence microscopy. Average fluorescence per nucleus was determined and is shown in the box and whiskers plot. The experiment was performed in duplicate and repeated 3 times.

Figure S3. miR-542-5p targets in the TGF-β signalling pathway

A. miR-walk 2.0 was searched with the hsa-miR-542-5p selecting all available databases. mRNAs targeted in at least 3 different databases were compiled and those in the TGF-β signalling pathway identified. TGF-β signalling is initiated by the binding of ligand to a receptor complex involving a TGFβ type I and TGFβ type II receptor. This binding increases

the serine-threonine kinase activity of the receptor complex leading to phosphorylation of SMAD2/3 at the C-terminal domain of the molecule, allowing multimerisation with the co-SMAD; SMAD-4 to form a trimeric complex of 2 SMAD2/3 and one SMAD4 (shown here for simplicity as a single SMAD2/3). This multimer can enter the nucleus where it functions as a transcription factor. The SMAD2/3 can also be phosphorylated in the linker region by several different kinases including Erk1 in a TAK1 dependent manner. This phosphorylation allows targeted degradation by NEDD4L so reduces overall SMAD signalling. Linker region phosphorylation can also occur in the nucleus as a consequence of CDK8/9 activity. The pathway is inhibited by the inhibition of the receptor complex by a heterodimer of SMAD7/SMURF1 which ubiquitinates the receptor. This heterodimer can also inhibit the formation of the SMAD2/3-SMAD4 dimer. SMAD2/3 function can also be inhibited by dephosphorylation by at least 2 different phosphatases, PP2A and PPM1A. The activity of these phosphatases contributes to the termination of pathway activity. Two other phosphatases also dephosphorylate SMAD2/3; CTDSP1 and CTDSP2. These proteins have been shown to dephosphorylate the linker region of SMAD2/3 and to increase SMAD signalling presumably by reducing degradation. The cycle of SMAD phosphorylation and de-phosphorylation is reviewed in (14, 15). The predicted targets of miR-542-5p included SMAD7, SMURF1, a catalytic component of PP2A (PPP2CA) and PPM1A suggesting that miR-542-5p would increase TGF-β signalling.

B. RNA was immunoprecipitated from cells transfected with miR-542-5p mimic or control mimic using anti-Ago2 as described in Supplementary Methods. Levels of SMAD7, SMURF1 and PPP2CA were quantified by PCR. SMAD7 was not robustly amplified and was present at low levels in the input controls. Data for SMURF1 and PPP2CA are presented as fold enrichment in the 542-5p transfected cells normalised to control transfected cells.

Figure S4. miR-542-5p increases basal nuclear phospho-SMAD2/3.

A. Top panel: Cells were transfected with miR-542-5p in the presence or absence of the antagomiR or with the control mimic. In all transfections oligo concentration was maintained by addition of control mimic. 2 days later cells were lysed and the protein was analysed by Western blotting for pSMAD2/3 before stripping the blot and reprobing for the unphosphorylated protein.

Lower panel: To confirm the result, cells were transfected with miR-542-5p or control mimic or left untransfected. 2 days later the untransfected cells were treated with 5ng/mL TGFβ1 for 2h before all the cells were harvested and the proteins analysed by western blotting. The ratio of phospo-SMAD2/3 to SMAD2/3 was determined by densitometry. Each sample value was normalized to the average density of the control transfected cells from that experiment. The data were then combined. Blue circles show data points from the lower panel and red diamond show data from the upper panel.

Consistent with the luciferase and immunofluorescence assays the phospho-SMAD:SMAD ratio was elevated the miR-542-5p transfected cells compared cells cotransfected with the antagomiR or transfected with the control mimic. Furthermore, the phospho-SMAD: SMAD ratio was highest in the cells treated with TGF-β.

B. Images from Figure 3 presented in colour to show overlap of DAPI and pSMAD2/3 staining. Left-hand images show DAPI staining for nuclei (Blue), the center images show pSMAD2/3 staining only (green), right hand images show a merge of pSMAD2/3 staining with DAPI.

Figure S5. SMAD7 is reduced by over-expression of miR-542 in mice

A. Fluorescent images showing regions of the *tibialis anterior* from mice electroporated with pCAGGS-EGFP or pCAGGS-542 as described in methods.

B. Fibre diameter and area were quantified in sections from the *tibialis anterior* of mice electroporated with pCAGGS-EGFP or pCAGGS-542. Fibre diameters above 15μm and below 70μm were binned into 5μm bins and fibre areas into 500μm^2 bins. There was a shift towards an increase in the proportion of smaller fibres in legs transfected with pCAGGS-542 compared to those transfected with pCAGGS-EGFP.

C. The *tibialis anterior* of mice was electroporated with pCAGGS-542 or pCAGGS as described in Methods. The muscle was harvested 3 days later and cytoplasmic extracts prepared. SMAD7 was immunoprecipitated from the cytoplasmic extract as described in Methods and analysed by western blotting. SMAD7 levels were reduced in miR-542 expressing muscles compared to those expressing EGFP alone.

Figure S6. Pre-operative miR-542-3p/5p expression is associated with hospital length of stay

Comparison of pre-surgery miR-542-3p (A) and miR-542-5p (B) expression with hospital length of stay (LOS) showed that both were positively correlated with poorer outcome (longer period hospitalized).

Figure S7. Pre-operative clinical associations with muscle wasting

Comparison of amount of muscle lost from the *rectus femoris* determined by ultrasound with pre-surgery cardiac function showed a weak negative correlation with LVEF% (A) and a weak positive correlation with age (B).

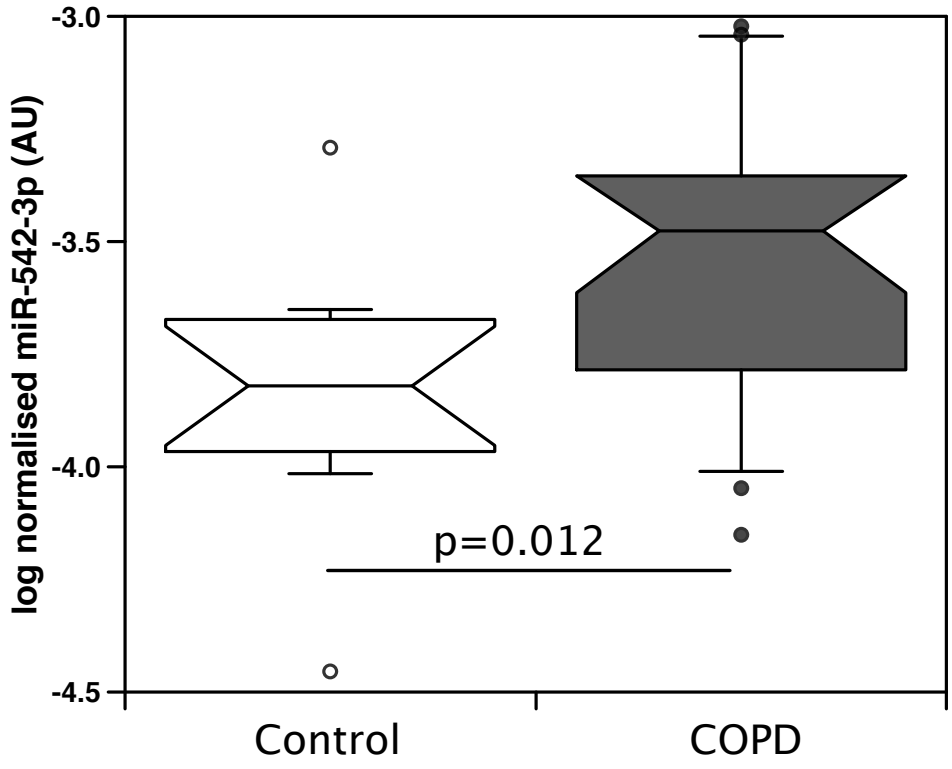

Figure S1

A

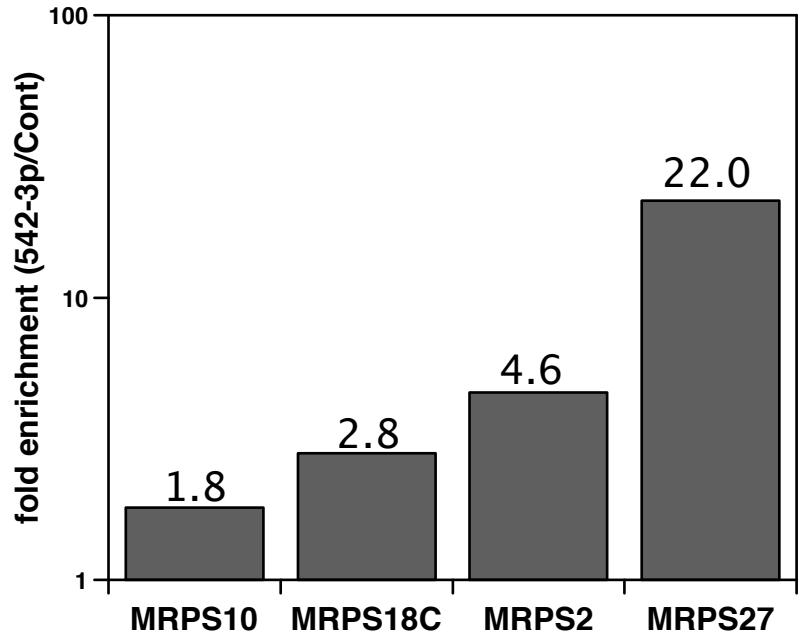

B

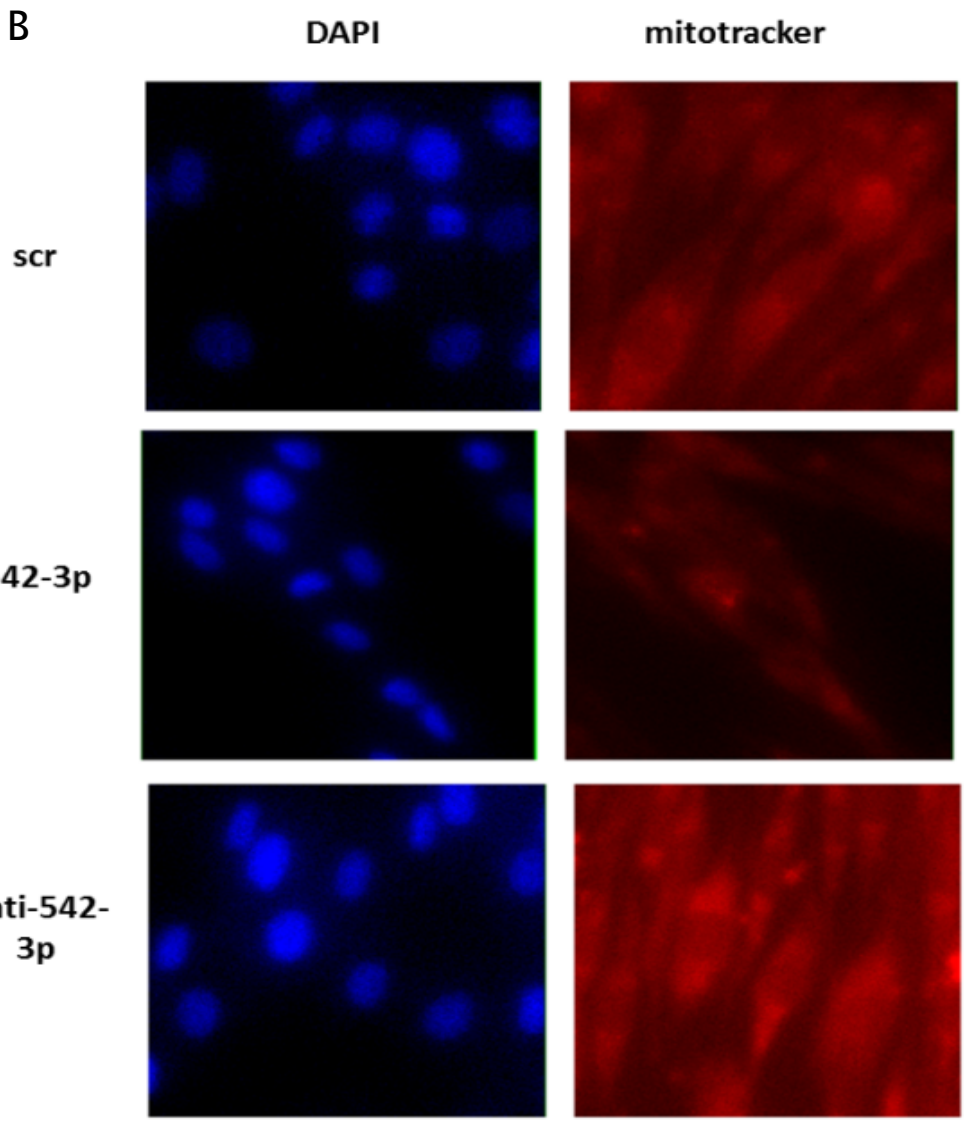

C

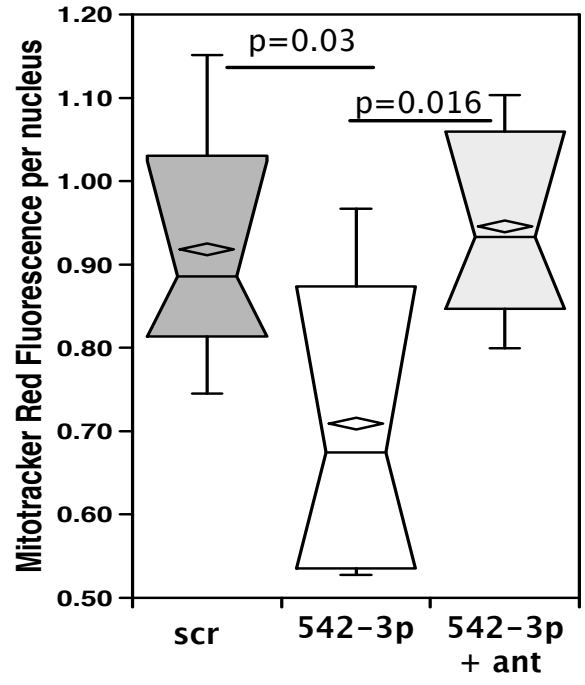

Figure S2

A

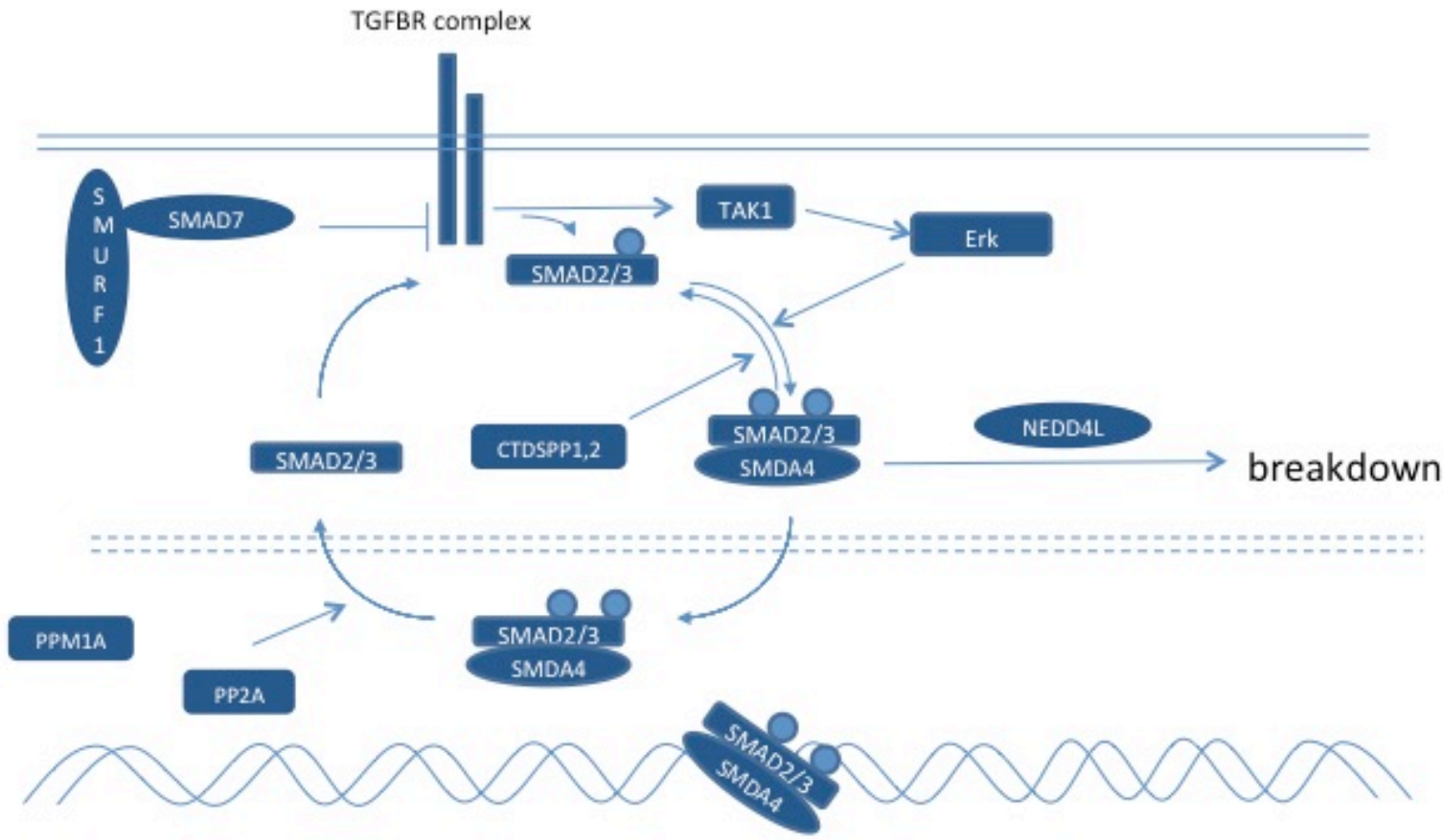
TGFBR complex
SMURF1
SMAD7
TAK1
Erk
SMAD2/3
SMAD2/3
CTDSPP1,2
SMAD2/3
SMDA4
NEDD4L
breakdown
PPM1A
PP2A
SMAD2/3
SMDA4
SMAD2/3
SMDA4

B

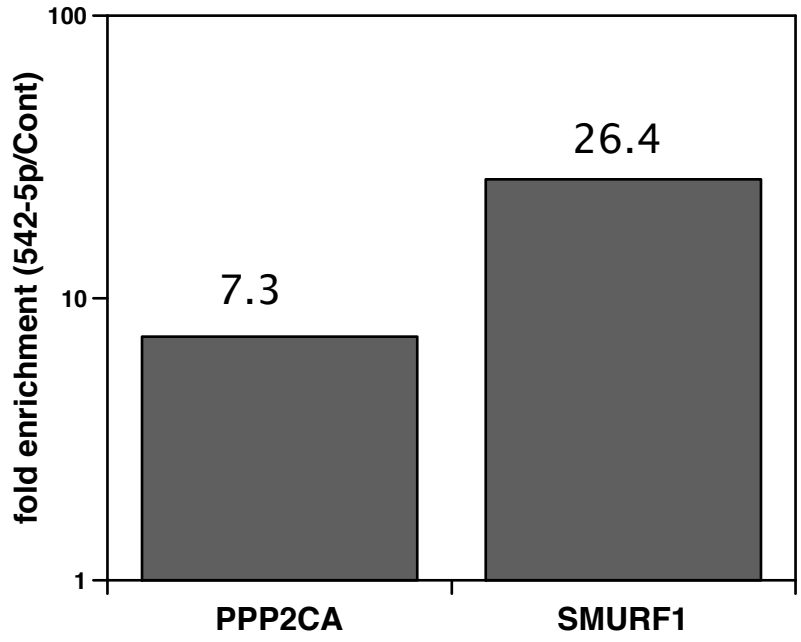
100
10
1
fold enrichment (542-5p/Cont)
7.3
26.4
PPP2CA
SMURF1

Figure S3

A

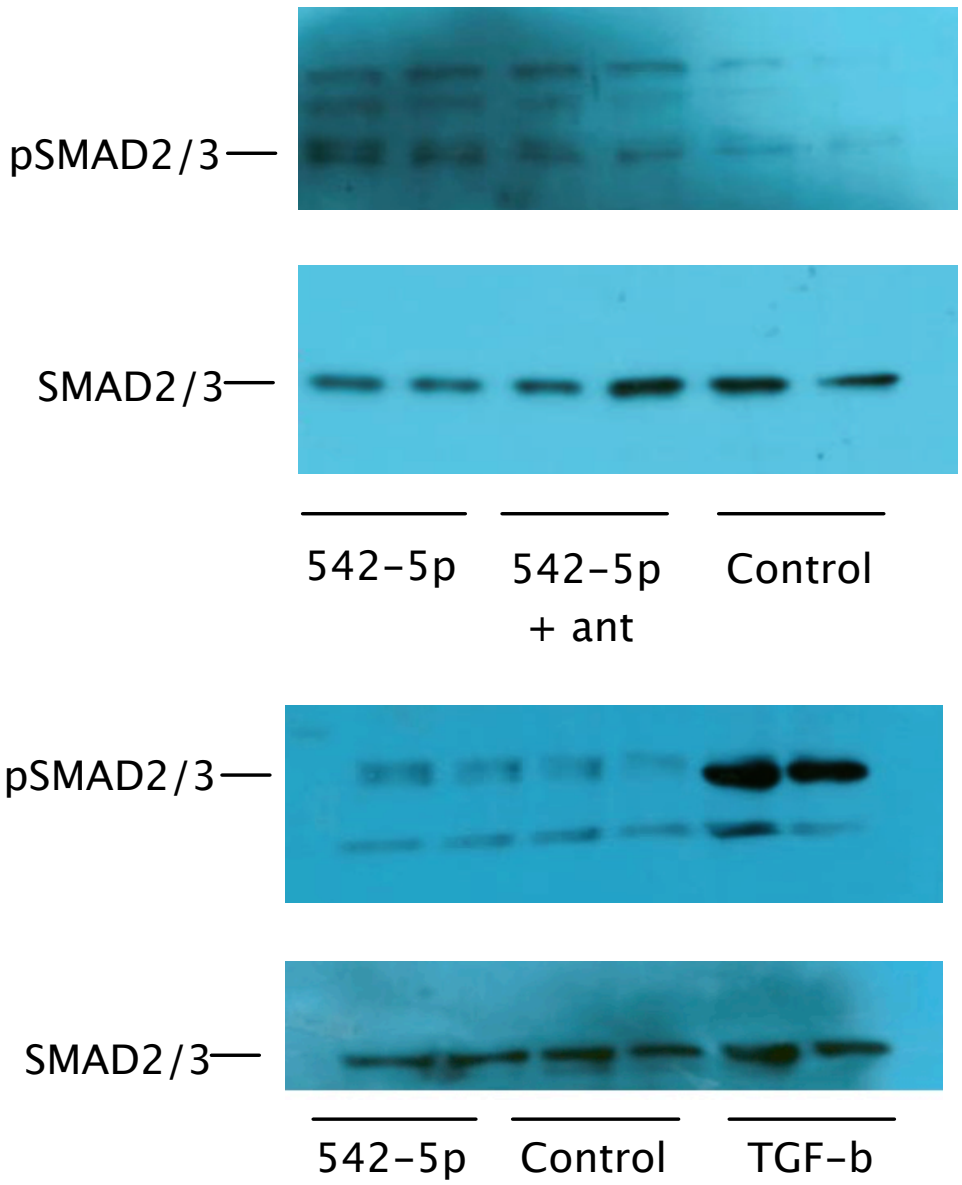
pSMAD2/3
SMAD2/3
542-5p
542-5p + ant
Control
pSMAD2/3
SMAD2/3
542-5p
Control
TGF-b

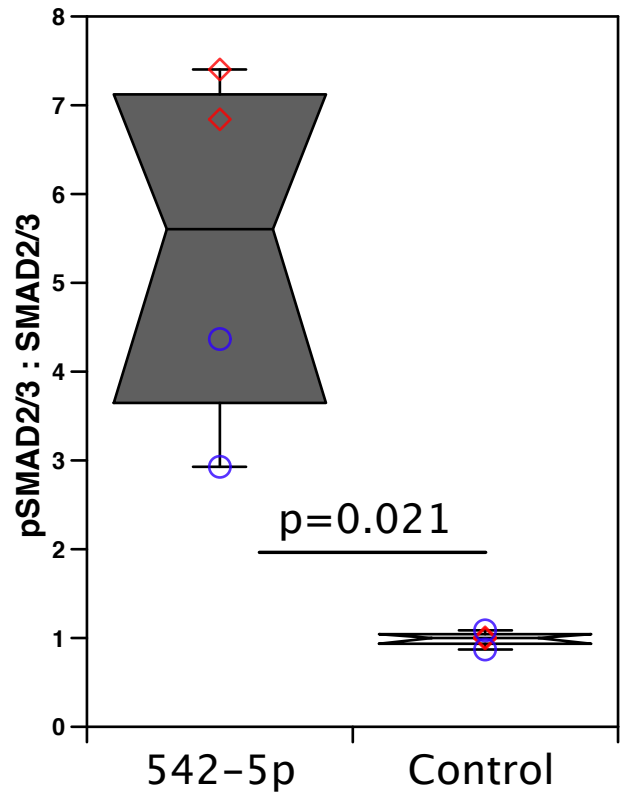
pSMAD2/3 : SMAD2/3
0
1
2
3
4
5
6
7
8
p=0.021
542-5p
Control

B

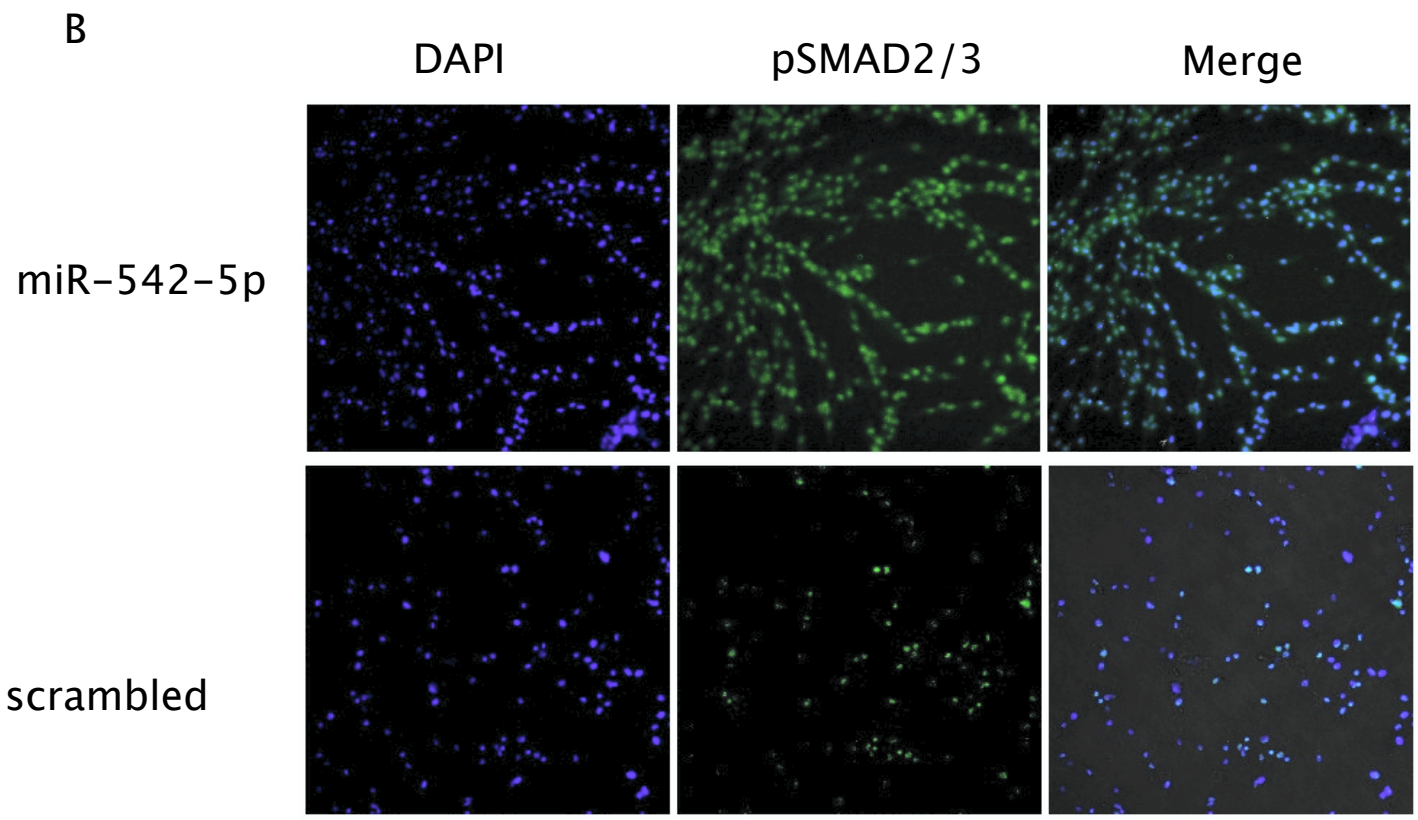
DAPI
pSMAD2/3
Merge
miR-542-5p
scrambled

Figure S4

A

pCAGGS

pCAGGS-542

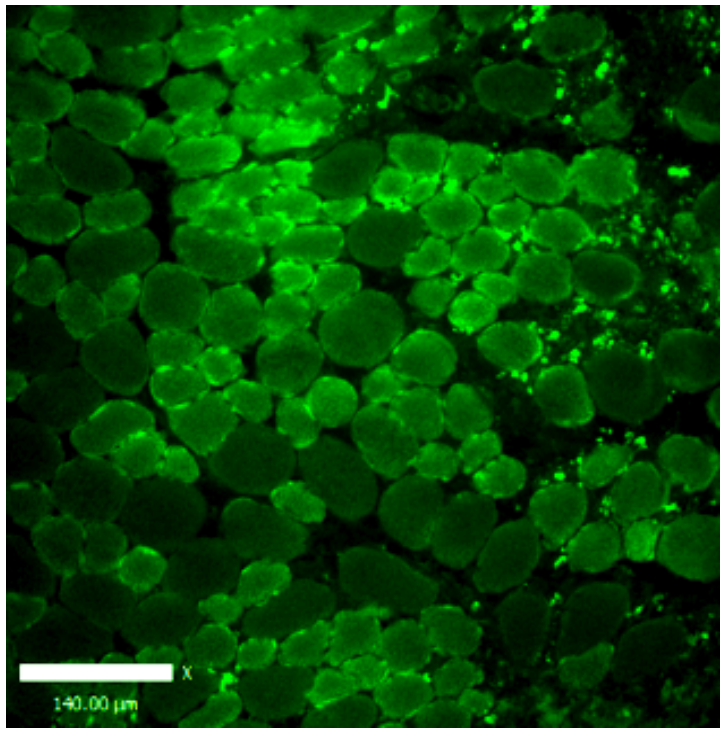

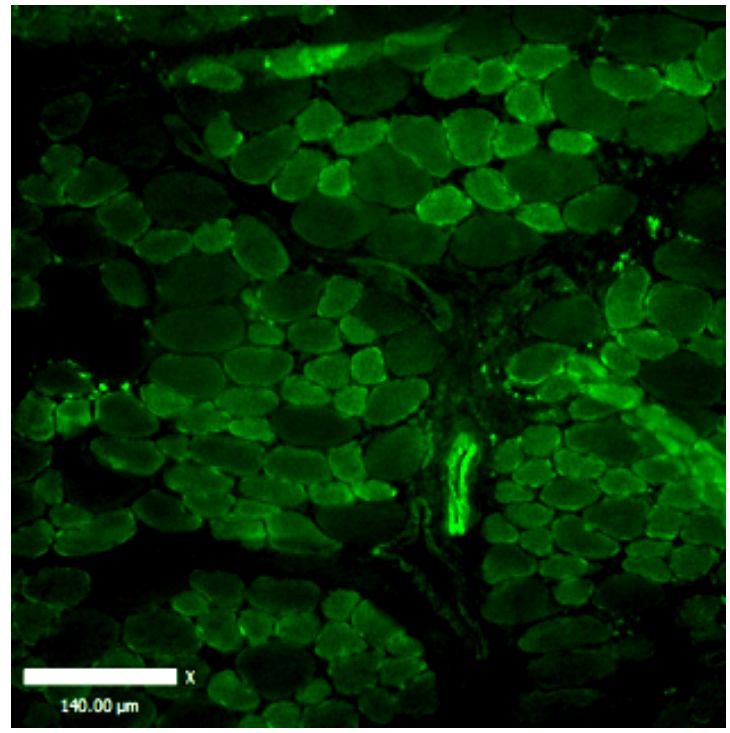

B

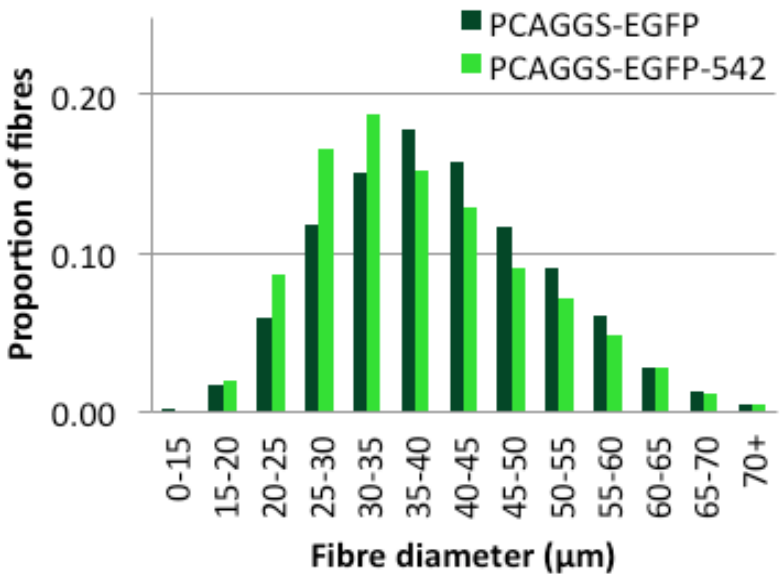

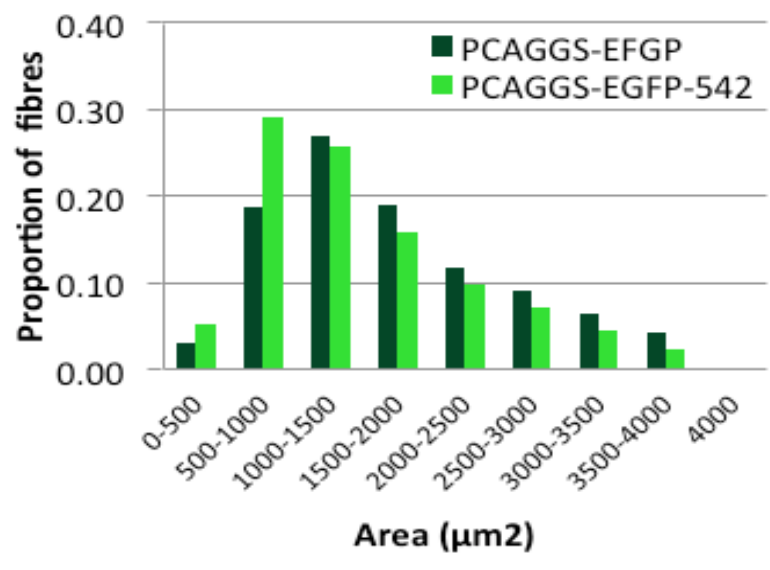

C

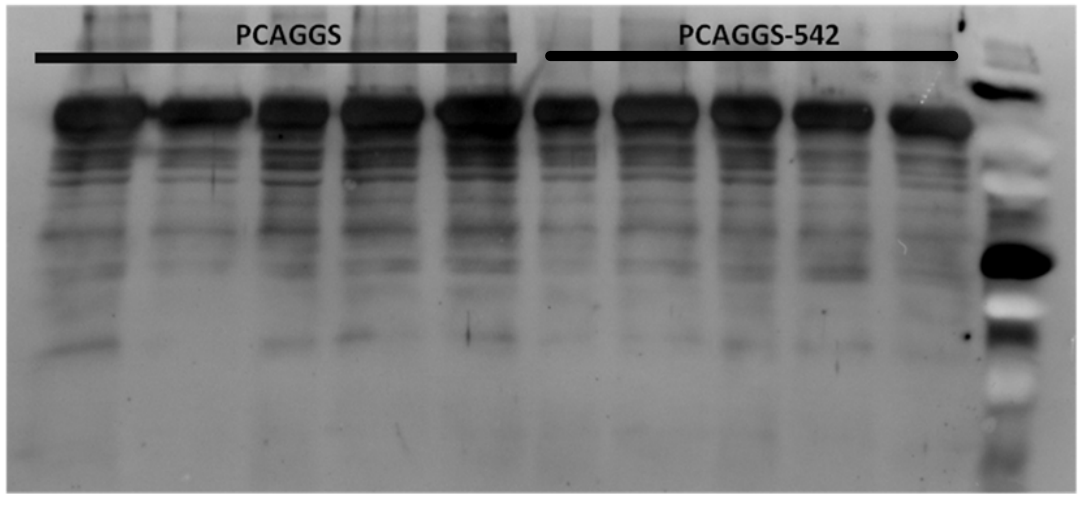

FIgure S5

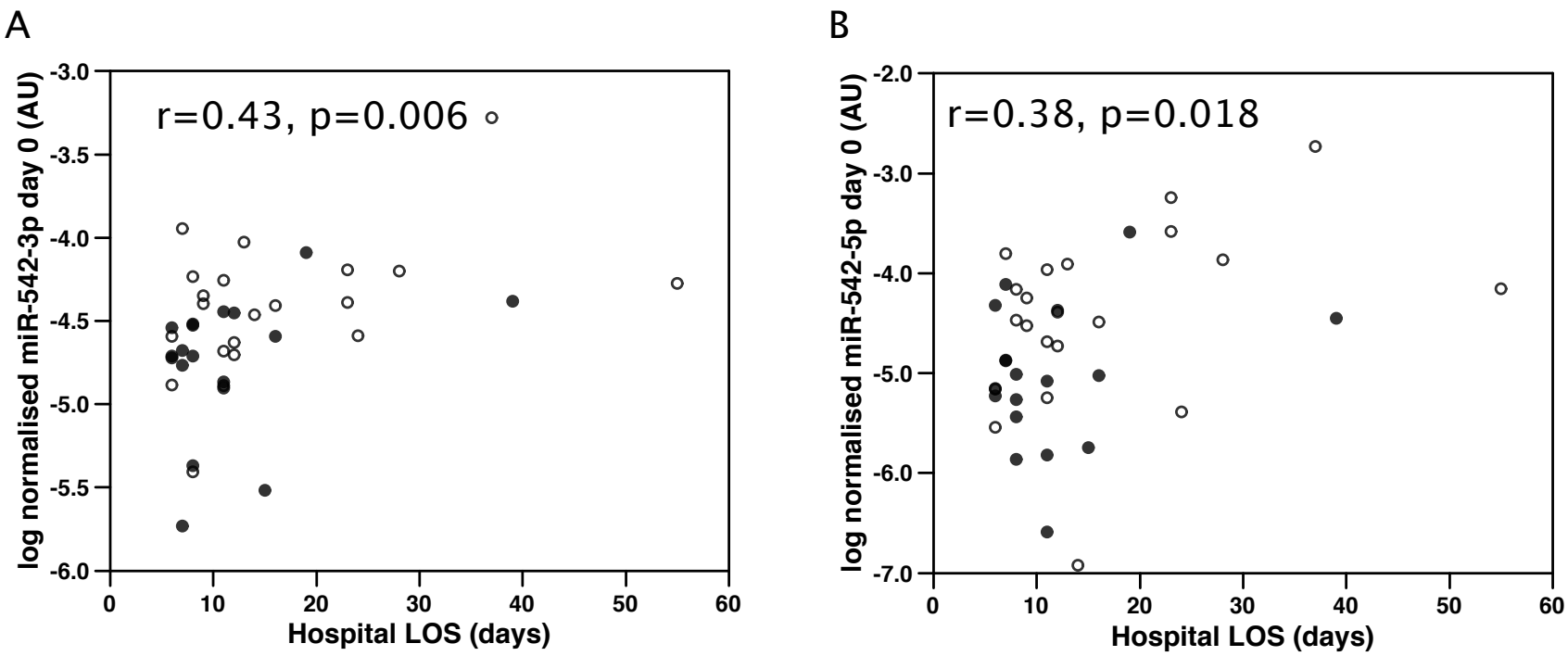
A
r=0.43, p=0.006
log normalised miR-542-3p day 0 (AU)
-3.0
-3.5
-4.0
-4.5
-5.0
-5.5
-6.0
0
10
20
30
40
50
60
Hospital LOS (days)
B
r=0.38, p=0.018
log normalised miR-542-5p day 0 (AU)
-2.0
-3.0
-4.0
-5.0
-6.0
-7.0
0
10
20
30
40
50
60
Hospital LOS (days)

Figure S6

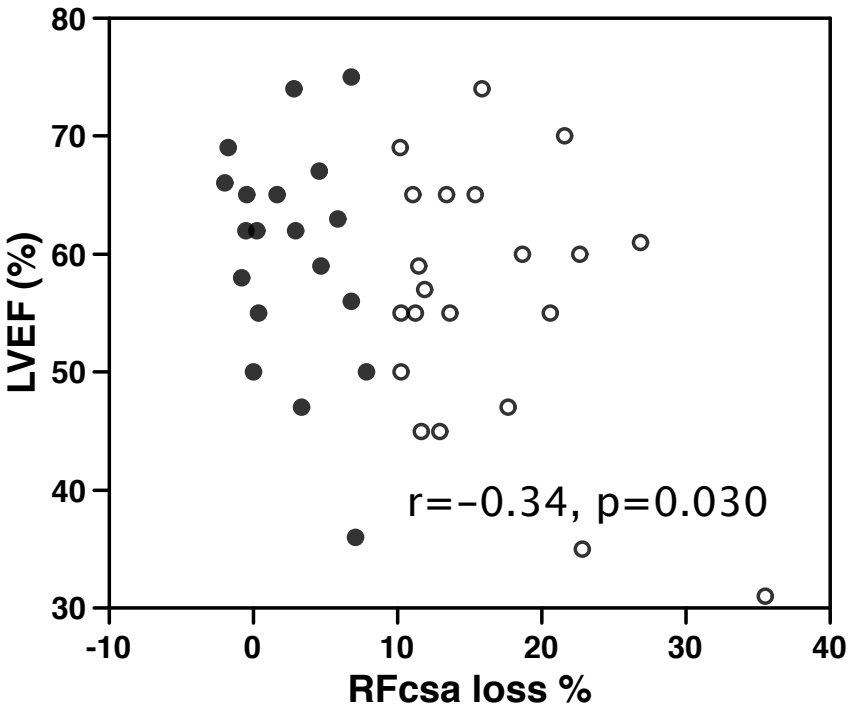

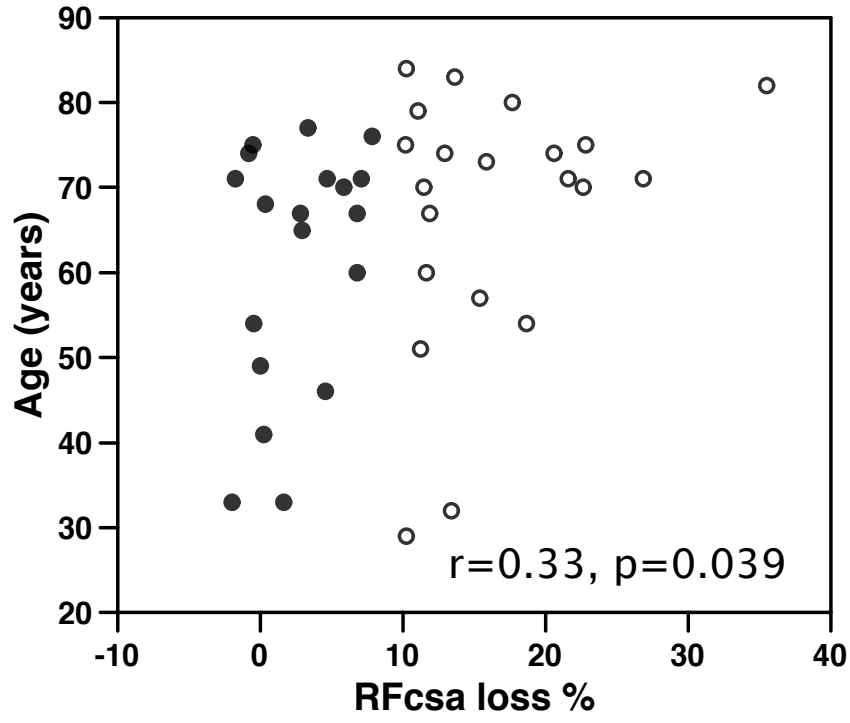

Figure S7

Supplementary Table 1: Physiological characteristics of the screen cohort

	Control (n=7)	COPD (n=14)
Age (years)	67 ± 11	66 ± 6
Smoking History[a] (pack-year)	6.25 (0, 24)	48 (34, 68)**
Weight [a] (kg)	75.5 (74.1, 86.8)	70.5 (60.8, 93.4)
BMI[a] (kg/m^2)	25.7 (24.8, 26.9)	23.8 (20.8, 26.2)
FFMI [a] (kg/m^2)	18.5 (17.5, 20.0)	15.9 (14.5, 17.0)*
FEV_1 [a] (% pred)	107.7 (104.0, 123.2)	29.6 (25.1, 35.5)***
TLCO [a] (% pred)	86.7 (84.5, 90.8)	29.5 (26.2, 54.2)
6min walk % pred	116 ±12	66 ±27***
SGRQ [a]	1 (0, 8)	56 (49, 69)***
Quadriceps MVC (kg)	39.9±6.6	29.8 ± 8.6*
Quadriceps MVC (% pred)	77 ± 15	60± 13*
Locomotion time[a] (min/12 hr)	90 (67, 115)	47 (17, 71)

BMI (Body mass index), FFMI (fat free mass index), FEV_1 (Forced expiratory volume in 1 sec), RVTLC (ratio of the reserve volume to total lung capacity), TLCO (transfer capacity of the lung for CO) SGRQ (St George's respiratory questionnaire) MVC (maximal voluntary contraction). * $p<0.05$, ** $p<0.01$, ***$p<0.001$. Data are presented as mean ±SD for normally distributed data or as median (interquartile range) for data that was not normally distributed

Supplementary Table 2: Physiological characteristics of the COPD validation cohort

	Control (n=12)	COPD (n=24)
Age (years)	67 ± 8	66 ± 10
Smoking History[a] (pack-year)	7 (0,25)	40 (29,59)***
Weight [a] (kg)	83 ± 15	68 ± 12**
BMI[a] (kg/m^2)	26.3 (24.8, 28.7)	22.4 (21.1, 24.4)**
FFMI [a] (kg/m^2)	19.0 (17.2, 20.6)	15.9 (14.7, 16.9)***
FEV_1 [a] (% pred)	107.6 (100.6, 116.8)	35.5 (27.5,42.5)***
TLCO [a] (% pred)	90.5 (84.5, 97.2)	42.7 (29.7,52.3)***
6min walk (% pred)	121±14	75±20***
SGRQ [a]	2 (0, 8)	53 (43, 66)***
Quadriceps MVC (kg)	41±9	31 ± 8**
Quadriceps MVC (% pred)	82±20	66 ± 14*
Locomotion time[a] (min/12 hr)	90 ± 33	43 ± 25***

BMI (Body mass index), FFMI (fat free mass index), FEV_1 (Forced expiratory volume in 1 sec), RVTLC (ratio of the reserve volume to total lung capacity), TLCO (transfer capacity of the lung for CO) SGRQ (St George's respiratory questionnaire) MVC (maximal voluntary contraction). * $p<0.05$, ** $p<0.01$, ***$p<0.001$. Data are presented as mean ±SD for normally distributed data or as median (interquartile range) for data that was not normally distributed

Supplementary Table 3 Physiological characteristics of aortic surgery patients

	Non-wasting Patients (n=19)	Wasting Patients (n=21)	P-value
Demographic data			
Age (yr)	58.7 ± 15.4	68.1 ± 14.9	*
Sex (M/F)	17/4	17/7	
BMI (kg/m2)	27.1 ± 3.6	27.5 ± 6.9	NS
EuroSCORE 2	2.0 (1.3-3.5)	3.0 (1.4-9.6)	NS
Pre-operative LVEF (%)	59.6 ± 9.1	56.0 ± 10.6	NS
Pre-operative creatinine clearance (µmol/L)	74.1 ± 16.3	68.0 ± 20.4	NS
SPPB	12 (12,12)	10 (10-12)	***
WHO performance status			
Pre-operative	0 (0-1)	1 (0-1)	*
Post-operative	1 (0-2)	2 (1-3)	*
Operative data			
Total bypass time (mins)	143.0 ± 49.0	142.1 ± 55.7	NS
Total cross-clamp time (mins)	103.6 ± 35.4	95.7 ± 33.2	NS
Critical care data			
ICU length of stay, days	1.0 (1-2)	3.0 (2-7)	***
Hospital length of stay, days	8 (7-12)	12 (9-23)	*
Mechanical ventilation (hours)	16 (13-24)	26 (19-99)	**
Vasopressor duration (hours)	27 (15-48)	46 (22-186)	*

BMI (Body mass index), LVEF (left ventricular ejection fraction), SPPB (Short physical performance battery). * $p<0.05$, ** $p<0.01$, ***$p<0.001$. Data are presented as mean ±SD for normally distributed data or as median (interquartile range) for data that was not normally distributed

Table S4: Primers used in this study

Gene	Forward	Reverse
12S rRNA	CCCAAACTGGGATTAGATACCC	GTTTGCTGAAGATGGCGGTA
16S rRNA	GCCTGTTTACCAAAAACATCAC	CTCCATAGGGTCTTCTCGTCTT
Human SMURF1	TCGTGAGTTTATTGCATATGTAACA	CTTCCCACTGTTTTTATCACTGA
Human PPP2CA	TGGTGGTCTCTCGCCATCTA	CATTGGACCCTCATGGGGAA
Human SMAD7	TCGGACAGCTCAATTCGGAC	GGTAACTGCTGCGGTTGTAA
Human CTDSP1	GACCCCAGTCCAATACCTGC	TCACTGGCTTGAAGGAGCTG
Human CTDSP2	GCCAGTCAAGTTCCTCCACT	GTCCCTGGGATCTGGTAGAA

References

1. Natanek SA, Gosker HR, Slot IG, Marsh GS, Hopkinson NS, Man WD, Tal-Singer R, Moxham J, Kemp PR, Schols AM, Polkey MI. Heterogeneity of quadriceps muscle phenotype in chronic obstructive pulmonary disease (Copd); implications for stratified medicine? *Muscle Nerve* 2013; 48: 488-497.
2. Rabe KF, Hurd S, Anzueto A, Barnes PJ, Buist SA, Calverley P, Fukuchi Y, Jenkins C, Rodriguez-Roisin R, van WC, Zielinski J. Global strategy for the diagnosis, management, and prevention of chronic obstructive pulmonary disease: GOLD executive summary. *AmJRespirCrit Care Med* 2007; 176: 532-555.
3. Wanger J, Clausen JL, Coates A, Pedersen OF, Brusasco V, Burgos F, Casaburi R, Crapo R, Enright P, van der Grinten CP, Gustafsson P, Hankinson J, Jensen R, Johnson D, Macintyre N, McKay R, Miller MR, Navajas D, Pellegrino R, Viegi G. Standardisation of the measurement of lung volumes. *EurRespirJ* 2005; 26: 511-522.
4. Steiner MC, Barton RL, Singh SJ, Morgan MD. Bedside methods versus dual energy X-ray absorptiometry for body composition measurement in COPD. *EurRespirJ* 2002; 19: 626-631.
5. ATS statement: guidelines for the six-minute walk test. *Am J Respir Crit Care Med* 2002; 166: 111-117.
6. Bergstrom J. Percutaneous needle biopsy of skeletal muscle in physiological and clinical research. *Scand J Clin Lab Invest* 1975; 35: 609-616.
7. Bloch SA, Lee JY, Syburra T, Rosendahl U, Griffiths MJ, Kemp PR, Polkey MI. Increased expression of GDF-15 may mediate ICU-acquired weakness by down-regulating muscle microRNAs. *Thorax* 2015; 70: 219-228.
8. Seymour JM, Ward K, Sidhu PS, Puthucheary Z, Steier J, Jolley CJ, Rafferty G, Polkey MI, Moxham J. Ultrasound measurement of rectus femoris cross-sectional area and the relationship with quadriceps strength in COPD. *Thorax* 2009; 64: 418-423.
9. Ellis PD, Smith CW, Kemp P. Regulated tissue-specific alternative splicing of enhanced green fluorescent protein transgenes conferred by alpha-tropomyosin regulatory elements in transgenic mice. *J Biol Chem* 2004; 279: 36660-36669.
10. Gollins H, McMahon J, Wells KE, Wells DJ. High-efficiency plasmid gene transfer into dystrophic muscle. *Gene Ther* 2003; 10: 504-512.
11. McMahon JM, Signori E, Wells KE, Fazio VM, Wells DJ. Optimisation of electrotransfer of plasmid into skeletal muscle by pretreatment with hyaluronidase -- increased expression with reduced muscle damage. *Gene Ther* 2001; 8: 1264-1270.
12. Dweep H, Sticht C, Pandey P, Gretz N. miRWalk--database: prediction of possible miRNA binding sites by "walking" the genes of three genomes. *J Biomed Inform* 2011; 44: 839-847.
13. Bloch S, Lee JY, Wort SJ, Polkey MI, Kemp P, Griffiths M. Sustained elevation of circulating GDF-15 and a dynamic imbalance in mediators of muscle homeostasis are associated with the development of acute muscle wasting following cardiac surgery. *Crit Care Med* 2013; 41: 982-989.
14. Bruce DL, Sapkota GP. Phosphatases in SMAD regulation. *FEBS Lett* 2012; 586: 1897-1905.
15. Wrighton KH, Feng XH. To (TGF)beta or not to (TGF)beta: fine-tuning of Smad signaling via post-translational modifications. *Cell Signal* 2008; 20: 1579-1591.